GEOLOGY AND MINERALIZATION IN THE DUNKA ROAD COPPER-NICKEL MINERAL DEPOSIT, ST. LOUIS COUNTY, MINNESOTA

by

Stephen Geerts, Randal J. Barnes* and Steven A. Hauck

March 1990

Technical Report
NRRI/GMIN-TR-89-16

Funded by the Greater Minnesota Corporation

Natural Resources Research Institute
University of Minnesota, Duluth
5013 Miller Trunk Highway
Duluth, Minnesota 55811

*Dept. Civil and Min. Engineering
University of Minnesota
500 Pillsbury Drive S.E.
Minneapolis, Minnesota
55455

ABSTRACT

The Dunka Road Cu-Ni deposit is within the Partridge River Intrusion (T. 60 W., R. 13 W.), which is part of the Duluth Complex, and is approximately 1.1 b.y. (Keweenawan) in age. Relogging of 46 drill holes at the Dunka Road Cu-Ni deposit identified four major lithologic units and several internal ultramafic subunits that can be correlated over two miles. The ultramafic subunits (layers of picrite to peridotite) exhibit relative uniform thicknesses and are present at the same relative elevation within the major lithologic units. The major lithologic units, the same as delineated by Severson and Hauck (1990), and upward from the basal contact are: Unit I, a fine- to course-grained a sulfide-bearing troctolite to pyroxene troctolite (450 ft. thick) with associated ultramafic layers I(a), I(b), and I(c); Unit II, a medium- to coarse-grained troctolite to pyroxene troctolite (200 ft. thick) with a basal ultramafic layer II(a); Unit III, a fine-grained, mottled textured troctolitic anorthosite to anorthositic troctolite (150 ft. thick) with one minor ultramafic layer III(a); and Unit IV, a coarse-grained troctolite/pyroxene troctolite to anorthositic troctolite with associated ultramafic layers IV(a) and IV(b).

Most sulfide mineralization occurs within Unit I. Within Unit I the sulfide mineralization is both widespread but variable in modal percentage (rare to 5%), continuity and thickness (few inches to tens of feet). Sulfide mineralization is somewhat related with proximity to: hornfels inclusions, the basal contact with the footwall Virginia Formation, and some of the internal ultramafic layers within Unit I. Precious metal mineralization (Pd+Pt+Au) is associated with fracturing and alteration of the host rocks. The alteration assemblage is chlorite, bleached plagioclase, serpentine and uralite.

Pd+Pt values range from 100 to >2400 ppb over 10 foot intervals. These intervals can occur independently as 10 to 50 foot zones, or as part of a larger correlatable

occurrence/horizon. Two mineralized subareas within the Dunka Road deposit are: 1) an area which is peripheral to a highly anomalous Pd occurrence (reported by Morton and Hauck, 1987; 1989) herein termed the "southwest area", and 2) the "northeast area" which contains several drill holes that have near surface intercepts of >1% Cu. There are four somewhat large mineralized occurrences within the study area that carry >300 ppb combined total Pt+Pd+Au. These mineralized zones appear to be stratigraphically controlled by the ultramafic subunits within Unit I. Three of the four correlatable zones are found within the southwest area, and range from 40 to 130 feet thick. High Pd values within these zones range from 10 to 20 feet thick with values of 800 to 1650 ppb Pd. In the northeast area, the fourth mineralized zone appears continuously throughout Unit I. This zone ranges from 120 to 300 feet thick. High Pd values within this zone range from 10 to 40 feet thick with values of 800 to 1500 ppb Pd. Many 5 to 30 foot intersections of >1 ppm Pd+Pt+Au occur throughout the mineral deposit.

Geostatistical analysis based on 72 vertical holes and 12 angle holes suggests: 1) the base of the complex is a critical datum with the higher grade intercepts located between 100 and 400 feet above the base; 2) high inter-element correlations support local redistribution/concentration of primary mineralization by a secondary hydrothermal process and thus, polymetallic mining selectivity is possible; 3) the available drilling gives a spacial range of geologic influence at 400 foot centers, but sufficient angle drilling is not available to assess the potential of high grade, steeply dipping mineralized zones; 4) additional vertical in-fill drilling will almost certainly not discover any additional quantity of ore within the volume of rock studied; but 5) additional angle drilling to assess the potential of high grade, steeply dipping, mineralized zones would benefit a more complete geostatistical analysis.

TABLE OF CONTENTS

LIST OF FIGURES

LIST OF PLATES

LIST OF TABLES

LIST OF APPENDICES

INTRODUCTION

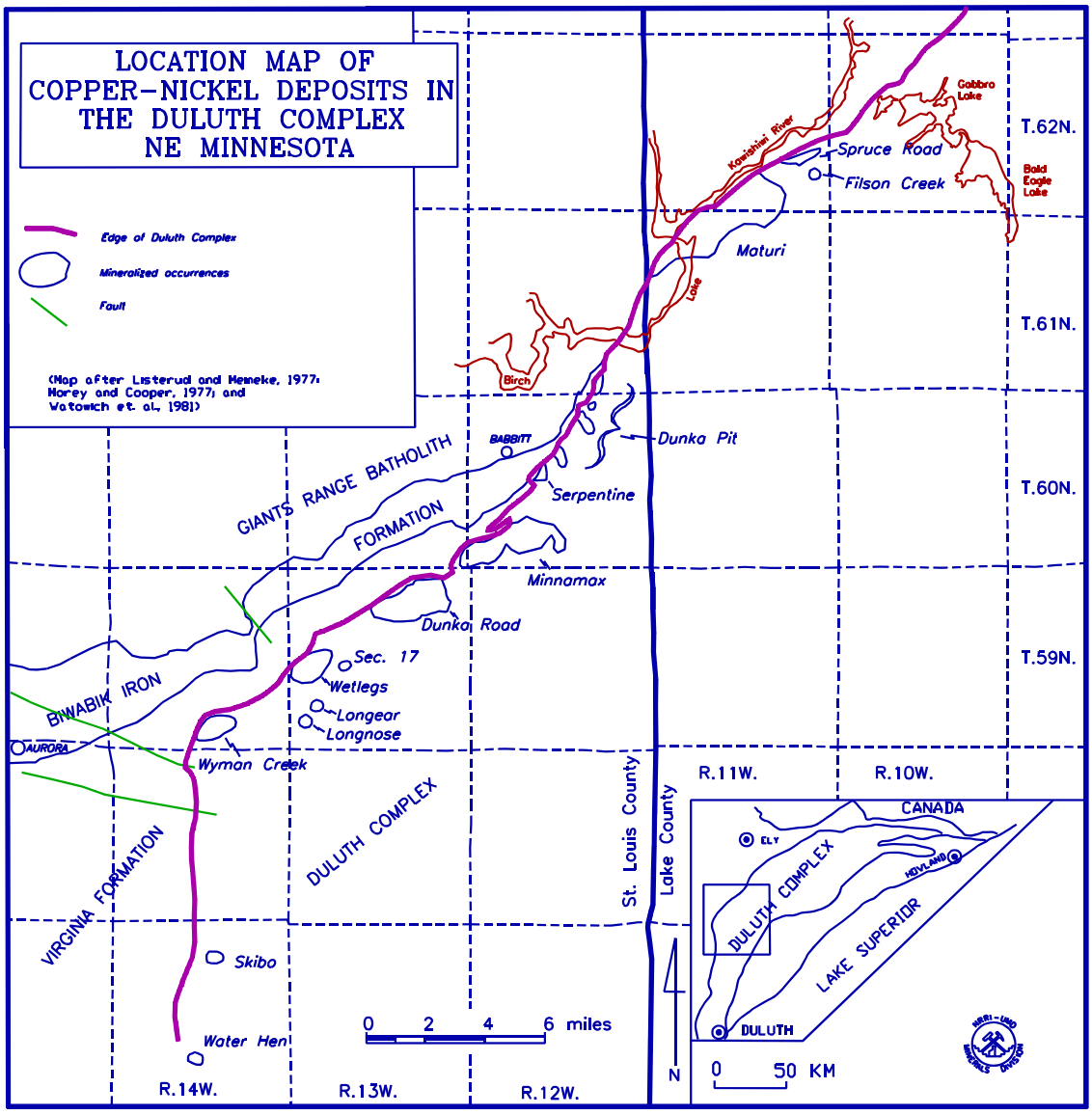

Figure 1. Location map of copper-nickel deposits in the Duluth Complex.

The Duluth Complex is located in northeastern Minnesota and consists of 1.1 b.y. Late Precambrian (Keweenawan) mafic and ultramafic intrusions. The Duluth Complex rocks are generally divided into an older anorthositic series (Davidson, 1972) and a younger troctolitic series (Bonnichsen, 1972). Within the later troctolitic series, three large intrusive bodies have been described. These intrusions are the South Kawishiwi

intrusion, the Partridge River intrusion, and the Bald Eagle intrusion (Foose and Weiblen, 1986). The Dunka Road copper-nickel mineral deposit occurs near the base of the younger troctolitic series rocks (T. 60 N., R. 13 W.) within the Partridge River intrusion (Fig. 1). Currently being reevaluated by Fleck Resources Ltd. (Vancouver, B.C.), the Dunka Road copper-nickel deposit was first discovered and drilled by U. S. Steel (USX) in the late 1960s. The purpose of this study was to: 1) construct a detailed stratigraphic/lithologic model for a portion of the Dunka Road Cu-Ni deposit; 2) determine the extent, quantity, and distribution of platinum group elements (PGEs), gold and silver content associated with the Cu-Ni mineralization; and 3) determine possible ore controls for the PGE-Au-Ag mineralization.

ACKNOWLEDGEMENTS

This project has been funded by GMC (Greater Minnesota Corporation). Special thanks are extended to USX and Mr. John McGoran (Fleck Resources Ltd.) for support and access to Dunka Road drill core and company records, i.e., assay data and drafted drill hole sections. Thanks are also extended Dr. Penelope Morton (UMD Geology Dept.) and to Mr. Mark Severson (NRRI) for their expertise and professional assistance with the Dunka Road project.

REGIONAL GEOLOGY

The geology of northeastern Minnesota is dominated by Precambrian age rocks; many of these rocks are Late Precambrian (1.1 b.y. - Keweenawan) and formed as a result of an intracontinental rifting. Due to the association with this rift system, the rocks of the Duluth Complex are the result of numerous, predominately mafic intrusions. The Duluth Complex extends northward from Duluth, Minnesota, in an arcuate belt, to just south of Ely, and then eastward toward Hovland, Minnesota (Fig. 1). The Duluth Complex is divided into an early anorthositic series (Davidson, 1972) and a later troctolitic series (Bonnichsen, 1972).

Along the western edge of the Duluth Complex, between Duluth and Ely, the troctolitic series is informally subdivided into three intrusions; the South Kawishiwi intrusion, the Partridge River intrusion and the Bald Eagle intrusion (Foose and Weiblen, 1986). The Dunka Road copper-nickel mineral deposit is at the northwestern contact of the Partridge River intrusion and the footwall rocks (Fig. 1). The footwall of the Partridge River intrusion consists of shallow dipping, Middle Precambrian (1.7 b.y.) metasediments of the Animikie Group. This group is composed of the Virginia Formation, Biwabik Iron-Formation and the Pokegama Quartzite.

The structure in the Duluth Complex is related to the Late Precambrian rifting event that formed the mid-continent rift system. According to Weiblen and Morey (1980), the formation of the Duluth Complex is directly related to the formation of a half-graben type model due to extensional tectonism. This model is dominated by steep southeast-dipping, northeast-trending normal faults that produced fractures and voids into which individual pulses of magma were emplaced. Also, Weiblen and Morey (1980) state that northwest-trending strike-slip (transform) faults were also formed during rifting.

DUNKA ROAD GEOLOGY

INTRODUCTION

Within the Partridge River intrusion, rocks are divided into eight separate and distinct rock units (Units I-VIII, Severson, 1988; Severson and Hauck, 1990). These rock units are composed primarily of troctolitic anorthosite to pyroxene troctolite, and in lesser amounts, gabbroic anorthosite to olivine gabbro (Fig. 2). However, due to the proximity of this study area to the basal (footwall) contact, only Severson and Hauck's (1990) first four rock units are present (Fig. 3; Plates 1 and 2). Initially, two subareas were singled out within the Dunka Road deposit: 1) an area, which is peripheral to a highly anomalous Pd occurrence (Morton and Hauck, 1987; 1989), herein termed the "southwest area"; and 2) the "northeast area" which contains several drill holes that have near surface intercepts of >1% Cu. The area of detailed study within the Dunka Road Cu-Ni deposit (Plate 1) includes 46 drill holes in these two localities along the northwestern border of the intrusion.

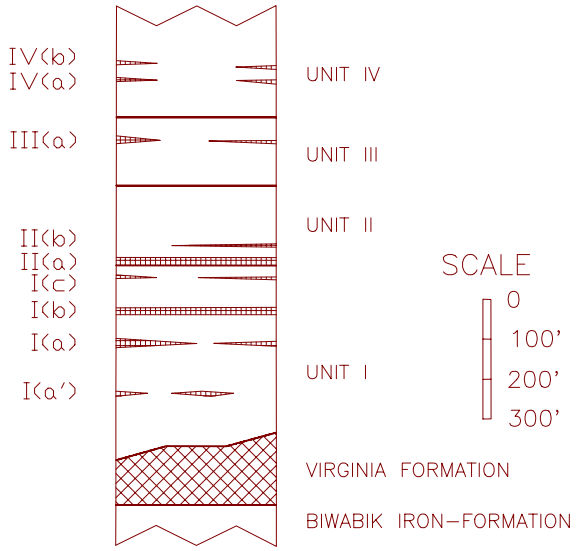

Figure 3. Generalized igneous "stratigraphic" section, Dunka Road Cu-Ni deposit.

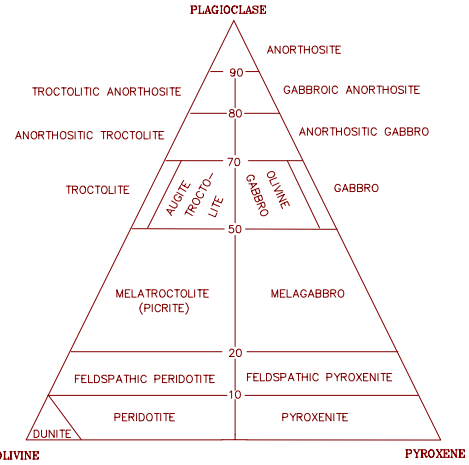

Figure 2. Rock classification for rocks in the Duluth Complex (after Phinney, 1972).

The southwestern area includes drill holes that were relogged between April and July, 1989. The northeastern area includes 15 drill holes plus drill holes between the two areas that were relogged between April and June, 1989 by J. Strommer. The surface area of the mineral deposit is approximately 4 square miles (only 1.5 sq. miles reevaluated by this study), and is shown on Plate 1 with a geophysical grid. U.S. Steel used the grid to later conduct diamond drilling on approximately 600 foot centers. Most of the drill holes that were relogged are vertical and they range in depth from 162 feet to 1145 feet.

Both geologic plan maps and cross-sections were constructed to assist with the interpretation of the geology, not all of which are presented in this report. Of the 20 northwest-trending cross-sections and the 5 geologic plan maps constructed for this project, two of the northwest-trending cross-sections and one geologic plan map have been included as examples (Plates 2, 6 and 7). A two mile longitudinal cross-section was constructed across the study area using correlations of the major lithologic units (Units I-IV) and minor internal ultramafic subunits (Plate 3). This cross-section was constructed using an assumed 20 degree dip for the footwall rocks (Severson, 1988). The lithologic units were then projected onto the cross-section. Depending on which side of the cross-section line the drill holes occurred (line A-A', Plate 1), the drill holes were adjusted in elevation using the 20 degree dip.

Only four of Severson and Hauck's (1990) eight rock units are present in drill core (Appendix A), due to the relative shallow depth of the Partridge River intrusion near the footwall contact (base of the complex in the area of study ranging in depth from 83 to 1101 feet). Of these four units, Unit IV is only partially represented because only a few holes were collared in this unit. Based upon the copper and palladium distribution as seen by cross-section A-A' (Plates 4 and 5), there are two separate and distinct

mineralized areas, i.e., southwest and northeast. These two areas are discussed in detail later in the report. However, since the rock units in both areas are the same, the following lithologic unit descriptions apply to both areas.

ANIMIKIE GROUP

The footwall rocks in the Dunka Road area consist of the Biwabik Iron-Formation and the Virginia Formation of the Middle Proterozoic Animikie Group. The Virginia Formation is the footwall lithology for most of the deposit.

Biwabik Iron-Formation

Only the top 20 feet of the Biwabik Iron-Formation exist in a few of the deeper holes within the Dunka Road deposit. Three horizons are present in the upper slaty member of the Biwabik Iron-Formation. The upper A submember is composed of a light colored, coarse-grained, massive marble. The B submember, below submember A, is composed of a fine- to medium-grained, green, irregular bedded diopside and chert. Most of the Biwabik Iron-Formation in the study area is composed of the lower C submember that is composed primarily of massive, banded magnetite and chert. Due to the limited amount of drilling into the Biwabik Iron-Formation in this area, the thickness of submembers could not be accurately determined. Dips on undeformed bedding planes average 20 degrees.

Virginia Formation

Overlying the Biwabik Iron-Formation, the Virginia Formation in the Dunka Road area occurs as a downward-tapering wedge of metasediments that thins to the southeast (Andrews and Ripley, 1989). Because the Dunka Road Cu-Ni deposit is

located where the wedge is thickest, the Virginia Formation is present in all 46 of the holes. However, only 10 of the 46 drill holes intersect the underlying Biwabik Iron-Formation. Therefore, an estimate of the average thickness would not be accurate. Also, due to differential scouring and/or assimilation by the intruding magma, the thickness of the unit varies from 36 to 290 feet in the southwest area to 27 to 250 feet in the northeast area (Appendix A). Most of the rocks composing the Virginia Formation are fine- to medium-grained argillites and graphitic argillites. These argillites are often biotite-rich (5 to 10 percent). They also commonly exhibit deformation, which is illustrated by weak to strongly contorted bedding planes. Dips on remnant, undeformed bedding planes range from 15 to 25 degrees. The argillaceous units also contain interbeds of graywacke, siltstone and minor calc-silicate layers. Some calc-silicate beds occur as pitted, saccharoidal layers, 6 to 24 inches thick, with cherty contacts. These saccharoidal layers may prove useful as `marker beds' in a stratigraphic interpretation of the Virginia Formation. Minor mudstone and graywacke also have sharp contacts with the recrystallized argillite. The trace minerals cordierite (usually found near the footwall contact) and pyrrhotite (increasing toward the footwall contact and occurring as bands within argillites) are present in many drill holes. The basal contact of the Virginia Formation with the Biwabik Iron-Formation is usually sharp.

PARTRIDGE RIVER INTRUSION

Igneous rock identification for this study is based on estimated modal percentages of plagioclase, olivine and pyroxene (Fig. 2) for rocks in the Duluth Complex (after Phinney, 1972). Due to small lateral changes in the modal percentages of these minerals, a slight variation in the rock types within the rock units may be present from hole to hole. This is especially true for Unit I. Therefore the description of igneous rock

units in this report is generalized.

The unit descriptions also include detailed explanations of the individual ultramafic subunits or layers that are a major factor for intra-unit correlation. Generally, these ultramafic subunits range in composition from picrite to dunite and from melagabbro to pyroxenite (Fig. 2). Most of the ultramafic subunits are within the picrite to peridotite compositional range. These subunits often exhibit modal grading with increasing olivine content toward the subunits' basal contact. The upper contacts are diffuse while the basal contacts are abrupt and sharp. The subunits are labeled numerically and alphabetically, corresponding to the major rock unit in which they occur. The subunits are labeled in ascending order within the unit.

Unit I

Of the four rock units within the study area, Unit I is the only unit that contains significant sulfide mineralization. Unit I is also the most complex unit, with abundant ultramafic layers and hornfels inclusions. Overall, Unit I averages 450 feet thick, ranging from 380 to 535 feet in the southwest area to 370 to 485 feet in the northeast area. Although characterization of the rocks is difficult, a large percentage of the lithologies are medium- to coarse-grained, pyroxene troctolite with cumulate textures and composed of (50-70%) plagioclase, (20-40%) olivine and (10-20%) pyroxene (Fig. 2). Grain size fluctuates dramatically throughout the unit, ranging from very fine-grained (<1 mm) to very coarse-grained (>5 mm). These grain size changes do not consistently correspond to any particular rock type. The rock type at the basal contact, from drill hole to drill hole, varies from a pyroxene troctolite to a norite and occasionally gabbro. These basal igneous lithologies are usually very fine-grained, and often show evidence of assimilation of the footwall Virginia Formation, i.e., rounded and partially dissolved

hornfels inclusions and a noticeable increase in fine-grained biotite content. Even though some evidence of assimilation is usually visible, in addition to the abundant hornfels inclusions, the contact between the Duluth Complex and the Virginia Formation is usually sharp. The most variable contacts within Unit I are the contacts between different igneous rock lithologies. These internal contacts range from abrupt to gradational and can occur over distances of one foot to tens of feet. The ultramafic layers can be correlated between drill holes with some degree of certainty, and thus the troctolitic rocks between the ultramafic layers also can be correlated. In some instances, a particular troctolitic rock name assigned to a specific interval may not exhibit a straightforward correlation with the same horizon in an adjacent drill hole due to a local lateral variation in the modal percentage of olivine or pyroxene in the parent rock.

Ultramafic Subunits. Three laterally continuous ultramafic subunits or layers have been identified within Unit I along with several discontinuous layers. These subunits are composed primarily of varying modal percentages of plagioclase (10-50%), olivine (50-90%) and pyroxene (usually <5%), and lesser amounts of oxides (magnetite/ilmenite <5%) and trace sulfides. The olivine content increases from top to bottom, e.g., picrite top to a peridotite base. Similarly, the contacts are usually gradational at the top and sharp on the bottom. The ultramafic subunits have an internal foliation represented by fracture cleavages that have average dips of 20 degrees.

Subunit I(a). Subunit I(a) is the lowest ultramafic horizon and occurs beneath I(b) and about 250 feet above the basal contact. This subunit is discontinuous on a hole by hole basis but occurs in both areas. In the northeast area, I(a) contains a higher percentage of pyroxene (30-50%) than olivine (10-20%). The composition of layer I(a),

therefore, varies from picrite to melagabbro. The subunit ranges in thickness from 4 to 20 feet thick in the southwest to 3 to 12 feet thick in the northeast.

Subunit I(b). Subunit I(b) is the most continuous of these layers and extends almost uninterrupted across the entire study area. Subunit I(b) is composed of a medium-to fine-grained picrite in the southwest and is from 1 to 18 feet thick. In the northeast area, I(b) varies from a fine-grained picrite to dunite with some minor melagabbro and ranges in thickness from 2 to 12 feet. This particular subunit occurs approximately 300 feet from the footwall contact in the southwest and 375 feet from the footwall contact in the northeast.

Subunit I(c). Approximately 425 feet above the footwall contact and above I(b), I(c) is present in only a few drill holes. This subunit is discontinuous but is present in both areas. The composition and thickness range from fine-grained picrite to feldspathic peridotite (3 to 5 feet thick) in the southwest to fine-grained picrite and peridotite (1 to 8 feet thick) in the northeast.

Several occurrences of very discontinuous ultramafic rock, e.g., I(a'), appear sporadically throughout the area within Unit I. These uncorrelatable ultramafic subunits or rocks are located below I(a). The only other occurrence of somewhat correlatable ultramafic rocks is within the southwest area. Located in drill holes 26021, 26039, 26017 and possibly 26047, is a tight, alternating sequence of ultramafic and troctolitic layers that is defined by intermixed intervals of 6 to 18 inch picrite and pyroxene troctolite layers. This entire sequence ranges from 25 to 50 feet thick and occurs about 200 feet above the basal contact.

Hornfels Inclusion. Although inclusions of Virginia Formation can be found at any elevation and within any of the rock units, the majority of the inclusions are located within Unit I. Many inclusions occur near the basal contact with the Virginia Formation. Hornfels inclusions range from a few inches up to 36 feet in diameter. Many of the inclusions are fractured and contain vein-like intrusions of troctolite. Inclusions near the basal contact are probably local in origin with minimal transportation. The inclusions are the result of intrusion of troctolite into fractures along bedding planes of the Virginia Formation.

These hornfels inclusions have experienced partial assimilation as evidence by gradational and often undefined contacts with the adjacent troctolitic rocks that contain an increased biotite content. The contacts exhibit varying degrees of chloritization and serpentinization within the contact zone. Due to partial assimilation and alteration of the inclusions, contacts are usually distorted or gradational. Mineralogically, the contact zone between Unit I and the Virginia Formation is generally higher in biotite and has a higher orthopyroxene to clinopyroxene ratio. Some inclusions, as well as the basal contact, are also associated with an increase in sulfide mineralization, usually as pyrrhotite. However, there is no apparent vertical or lateral correlation of the pyrrhotite mineralization from hole to hole.

Unit II

Unit II is characterized by homogeneous, medium- to coarse-grained troctolite and pyroxene troctolite with cumulate textures (Fig. 2) and a consistent basal ultramafic subunit, II(a) (Plates 3, 6 & 7). Mineralogically, Unit II is composed primarily of plagioclase (50-70%), olivine (20-40%), and pyroxene (0-10%). The continuity of the basal ultramafic subunit, in addition to the somewhat uniform grain size and

homogeneity of the troctolite, makes this unit easily distinguishable from Units I and III. Although the basal zone of Unit III can be gradational (decreasing olivine content upward), the upper contact of Unit II with Unit III is generally abrupt. The basal contact of Unit II with Unit I is usually sharp and recognized by: 1) the basal ultramafic subunit II(a); 2) lack of sulfides in Unit II; and 3) homogeneity of the main lithology in Unit II. The average thickness of Unit II is about 200 feet. The thickness, however, ranges from 110 to 250 feet in the southwest area to 120 to 240 feet in the northeast area.

The presence of sulfide mineralization within Unit II is generally rare and occurs as disseminated chalcopyrite and pyrrhotite. Most oxides present within Unit II occur as trace amounts of ilmenite and magnetite, which are most abundant within the ultramafic subunits II(a) and II(b).

Ultramafic Subunits. Two ultramafic subunits or layers have been identified in Unit II. These subunits range in composition from picrite to peridotite (Fig. 2), and are primarily composed of varying modal percentages of plagioclase (10-50%), olivine (50-90%), and pyroxene (usually <5%) with minor magnetite (usually <5%). The olivine in these ultramafic layers commonly increases toward the base, i.e., from picrite to peridotite. Also, associated with the increasing olivine content is increasing serpentinization and decreasing magnetic attraction (magnetite to hematite).

Subunit II(a). The basal ultramafic layer II(a) consists of medium- to fine-grained picrite to feldspathic peridotite and minor peridotite. There is little compositional change within the subunit from the southwest to northeast. The thickness in both areas ranges from 3 to 20 feet thick. A minor foliation, in the form of fracture cleavage, occurs within II(a). The foliation parallels the bedding plane and has a dip of 15 to 25 degrees.

Subunit II(a) also divides the unmineralized rocks of Unit II from the mineralized rocks of Unit I.

Subunit II(b). The second ultramafic subunit, II(b), which is composed of fine- to medium-grained picrite to felspathic peridotite in the southwest and coarser grained melagabbro in the northeast, is discontinuous throughout Unit II. This subunit ranges from 1 to 10 feet thick in the southwest and from 2 to 5 feet thick in the northeast. Subunit II(b) is generally located between 35 and 50 feet from the basal contact of Unit II. However, in the extreme northeast, the subunit is in proximity to the base of Unit III (approximately between 150 to 200 feet above the basal contact of Unit II).

Unit III

According to Severson (1988), Unit III is an excellent 'marker bed' in drill core. This unit is characterized by fine-grained troctolitic anorthosite to anorthositic troctolite with cumulate textures (Fig. 2) that range from 150 to 215 feet thick in the southwest to 140 to 175 feet thick in the northeast. Mineralogically, the unit is defined by plagioclase (70-90%) and poikilitic olivine (10-30%), which gives the rock an overall mottled appearance. Olivine occurs as random, 3 to 5 cm oikocrysts in a predominately plagioclase-rich groundmass. The plagioclase occurs as 3 to 5 mm, lath-shaped crystals. Clinopyroxene (0-5%) also often occurs as oikocrysts 3 to 4 cm in diameter that are randomly distributed.

The presence of sulfide mineralization is generally rare in Unit III, occurring as widely scattered and finely disseminated chalcopyrite and pyrrhotite. Also, rare oxides are usually associated with ultramafic occurrences as minor amounts of magnetite.

Ultramafic Subunit. The ultramafic occurrences within Unit III are sporadic and vary greatly in thickness and composition from hole to hole. One ultramafic layer has been identified and ranges in composition from picrite to melagabbro. Mineralogically, this layer is composed primarily of plagioclase (20-50%), olivine (25-40%), and pyroxene (25-40%) with minor amounts of magnetite (usually <5%).

Subunit III(a). Ultramafic subunit III(a) is discontinuous and inconsistent in thickness from hole to hole. Subunit III(a) is composed primarily of fine- to medium-grained picrite to melagabbro and may exhibit local weak serpentinization. This subunit ranges in thickness from 2 to 25 feet in the southwest but thins to 2 to 5 feet thick in the northeast. In the southwest area, the subunit is 100 feet above the basal contact of Unit III. However, in the northeast area, the subunit is only 30 to 40 feet from the basal contact of Unit III.

Unit IV

Unit IV is only partially represented in the study area and therefore, the thickness of this particular unit is unknown. However, the largest intersection of this unit is 245 feet in drill hole 26118 in the northeast area. Unit IV is characterized by coarse-grained, cumulate textured troctolite/pyroxene troctolite to anorthositic troctolite (Fig. 2). Unit IV has two discontinuous ultramafic subunits, IV(a) and IV(b), near the basal contact with Unit III (Plate 3). The most prominent difference between Units II and IV, other than being separated by Unit III, is Unit IV contains significant amounts of anorthositic troctolite and is coarser grained than Unit II. Sulfides in Unit IV are generally rare and occur as finely disseminated grains of chalcopyrite and pyrrhotite. Trace oxides are generally associated with the ultramafic layers. The oxides are fine-grained,

disseminated ilmenite and magnetite.

Ultramafic Subunits. In drill hole 26033, in the southwest area, both IV(a) and IV(b) occur as very coarse-grained (grain size 5-10 mm) melagabbro layers and have an average thickness of 1 and 3 feet, respectively. Similarly, these same subunits, approximately 5000 feet to the northeast in drill hole 26128, are more olivine-rich and occur as: IV(a), a fine-grained picrite layer (1.5 feet thick); and IV(b), a medium- to fine-grained layer grading upward from peridotite to picrite (5.5 feet thick). In both localities, the subunits occur from 100 to 150 feet from the basal contact of Unit IV. The subunits are separated by approximately 35 feet. These ultramafic layers, especially the more olivine-rich portions, often exhibit a foliation that parallels the bedding plane with dips of 15 to 20 degrees. Due to differing degrees of serpentinization, these layers may have varying degrees of magnetism.

STRUCTURE

Within the study area, the combination of gently dipping and variably assimilated basement rocks, and dramatic offsets in the basement rocks, complicates the structural interpretation in the Dunka Road deposit. However, offsets of ultramafic subunits and varying thicknesses of the individual igneous units document the presence of faulting. Two of these northeast-trending faults influence the stratigraphy of the study area (Severson and Geerts, unpub. data, 1989). These faults trend northeast and have a steeply dipping displacement to the southeast. The most dominant of these proposed faults is to the southeast of the study area and is represented by a major northeast-trending monoclinal and/or fault-like structure (Severson, 1988). This particular feature can be traced throughout the Dunka Road mineral deposit. The other postulated northeast-trending fault occurs as a series of displacements (independently offset in a northwest-southeast direction from grid line to grid line). The fault is located roughly half the distance between the monoclinal/fault feature and the surface intersection of the footwall rocks (Plates 6 and 7). Several northwest-trending strike-slip faults (Plates 2 and 3) can be explained by several unrelated offsets and Severson's (1988) basement contour map of the area. Severson's (1988) contour map on the top of the Biwabik Iron-Formation also supports these northwest-trending faults.

MINERALIZATION

SULFIDES AND PRECIOUS METALS

The sulfide mineralization in the northeast area of Dunka Road occurs throughout Unit I down to the basal contact. Unlike the northeast area, sulfide mineralization in the southwest area occurs sporadically in Unit I (Plates 4 and 5). In this area, the copper-nickel mineralization is generally concentrated near the middle of the unit, about 200 feet above the footwall contact. Between the two areas is a barren zone that extends from drill hole 26076 through 26047 (Plates 4 and 5). However, because of the limited number of drill holes in this area, the extent of this barren zone is unknown.

Sulfide distribution within Unit I is both sporadic and complex in that high and low Cu-Ni values cannot be correlated from hole to hole with any degree of certainty. The reasons for the lack of correlation may be: 1) the approximately 600 foot drill hole spacing in many areas; and 2) the distance of the sulfide mineralization from hornfels inclusions and/or the basal contact. There is a vertical change in the percentages of chalcopyrite and pyrrhotite in relationship to hornfels inclusions and/or the basal contact. The lateral change in these percentages may be similar but is not recognizable due to the wide drill hole spacing. The pyrrhotite to chalcopyrite ratio increases noticeably toward the contact with a hornfels inclusion and the basal contact of the Virginia Formation. A large number of hornfels inclusions in an area would, therefore, favor a higher percentage of pyrrhotite over chalcopyrite.

Sulfur isotope data suggests that most sulfur found in the deposit is of sedimentary derivation (Ripley and Al-Jassar, 1987). However, their study also indicates that *in situ* derivation is unlikely and that the sulfur was incorporated into the magma elsewhere, possibly an auxiliary magma chamber.

Mineralized zones containing Pd >800 ppb and/or zones with >1 percent Cu are considered to be, in this discussion, high grade. The host rocks of these high-grade zones are generally coarse-grained and range in composition from anorthositic troctolite to pyroxene troctolite. In the high grade zones, the amount of sulfide averages about 3 percent and has a range of 1-5 percent. In one extreme case, a zone of about 30 percent sulfides, the majority being chalcopyrite, is located in a 3 foot zone in hole 26010. This zone repeatedly assays >4 percent Cu and >10 ppm Pd and is considered to be related to a secondary or late-stage event (Morton and Hauck, 1989). The ratios of chalcopyrite to pyrrhotite in the high grade zones range from 3:1 to 5:1. The sulfide mineralization is generally disseminated and has grain sizes averaging 2-3 mm to massive sulfide.

Texturally, the sulfides are interstitial between subhedral plagioclase, olivine and pyroxene. The sulfides also occur as aggregates associated with the latter minerals in addition to biotite and/or ilmenite. Other minerals associated with this assemblage include pentlandite and apatite. The amount of oxides and biotite in these assemblages averages 1-2 percent. Most biotite occurs as 2 to 5 mm rims around the chalcopyrite. An estimated 50 to 60 percent of the sulfide accumulation at Dunka Road is represented by irregular sulfides associated with biotite (Ripley, 1981).

Although 10-50 foot thick zones of Pt+Pd+Au mineralization can occur independently, four large, but uneconomic, occurrences of Pt+Pd+Au mineralization can be correlated (ranging approximately 1150 ft. to 2650 ft. laterally) throughout the study area. These specific zones carry >300 ppb combined Pt+Pd+Au and appear to be stratigraphically controlled by ultramafic subunits over relatively large areas. These anomalous occurrences can generally be traced updip (northwest) to intersections in shallower holes. However, the Pt+Pd+Au occurrences near the top of Unit I often

intersect the surface before intersecting shallower holes (Plate 2). Downdip, these occurrences can be traced (southeast) to the edge of the study area. The extent to which these anomalies can be traced beyond the study area is unknown.

Three of the four occurrences are visible in the southwest area (Plate 4 and 5). The most evident occurrence is approximately 40 feet thick and occurs beneath ultramafic subunit II(a). This anomaly can be traced (northeast) 3000 feet along strike, from grid line 3320 SW to the northwest/southeast baseline (Plate 1). Within this occurrence is a 10-20 foot zone that runs 800 to 2100 ppb Pd (Plate 4). Another correlatable anomaly in the southwest area occurs beneath ultramafic subunit I(a) and is approximately 40 feet thick. This anomaly can be traced (northeast) to grid line 1298 SW. This anomalous zone also contains a 10 to 20 foot thick zone with Pd values of 800 to 1200 ppb. A third anomaly occurs between grid lines 1298 SW and 0. This occurrence ranges from 50 to 130 feet thick and has a 10 foot zone that assays 800 to 1200 ppb Pd.

In the northeast area, anomalous values of >300 ppb Pt+Pd+Au occur continuously throughout Unit I down to the basal contact. This anomalous zone ranges from 120 to 300 feet thick and can be traced (southwest) to grid line 2783 NE. Within this relatively large occurrence, two higher grade zones of Pd occur (Plate 4). One of these zones occurs beneath ultramafic subunit I(b) and ranges from 10 to 40 feet thick with values of 800 to 1500 ppb Pd. The other zone occurs between 50 and 100 feet above the basal contact. This Pd zone ranges from 10 to 30 feet thick with values of 800 to 1200 ppb Pd.

GEOCHEMISTRY

Seventeen hundred and seventy-three U.S. Steel pulps were reassayed by Fleck

Resources Ltd. for Cu-Ni-Pt-Pd-Au-Ag-Rh (Appendix C). These pulps represented previously split and assayed core (10 ft. intervals). One hundred and eighteen additional samples (Appendix C) from previously unsplit sulfide-bearing zones were assayed as a part of this project. These zones range in thickness from 1 to 5 feet. Both sample sets were assayed at Acme Labs in Vancouver, B.C. Cu-Ni-S data from the U.S. Steel drill program is also provided in Appendix C.

Several interesting relationships occur between Au-Ag-Cu-Ni-S and associated PGEs (Pt-Pd-Rh). While other correlations are possible, only a few of the relationships that best illustrate possible PGE ore controls are presented. Figures 4-9 illustrate several metal relationships (see Table 7 and 8 for correlation coefficients).

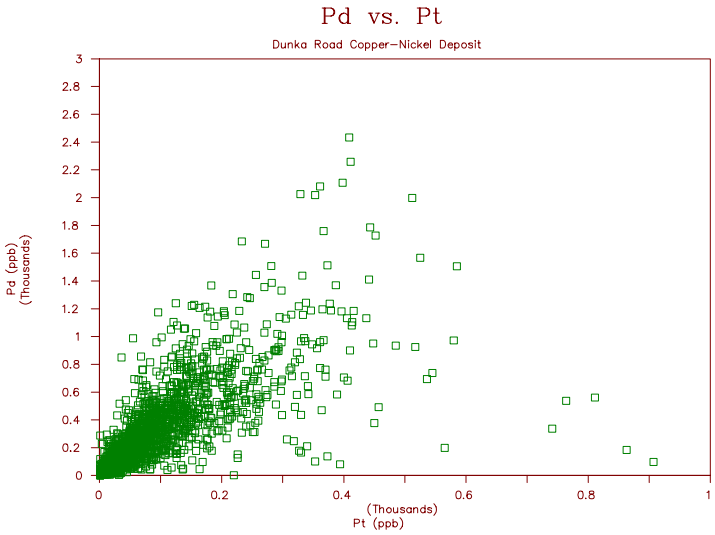

Figure 4. Platinum vs. Palladium

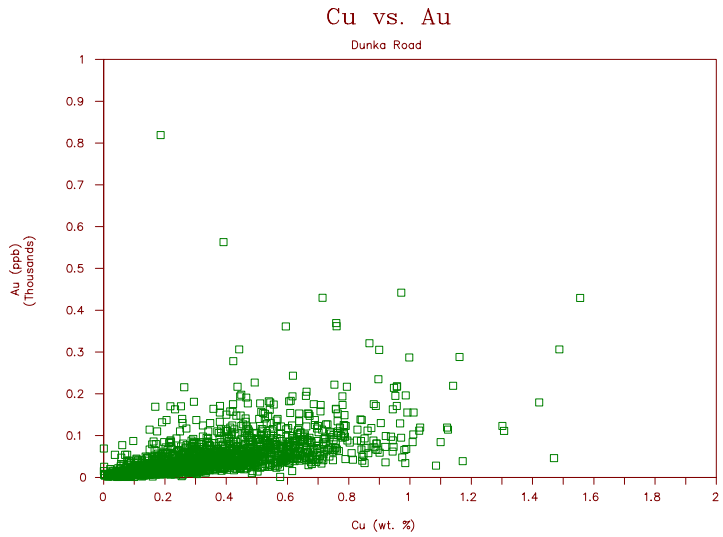

Figure 5. Copper vs. Gold

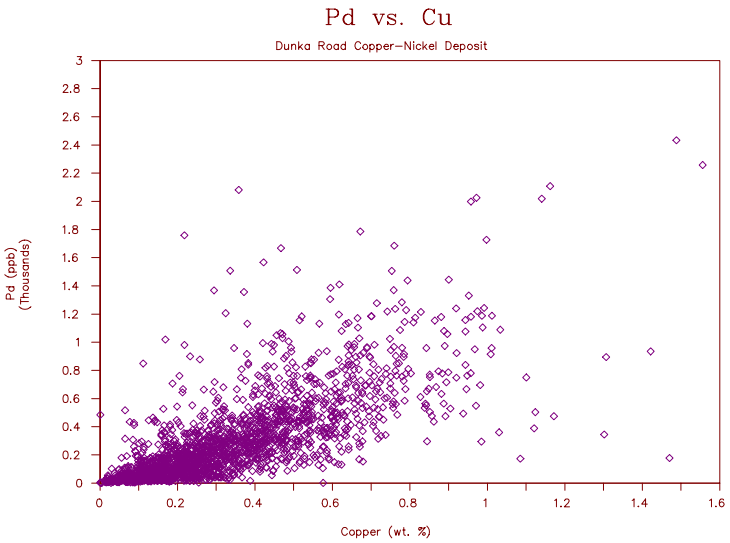

Figure 6. Copper vs. Palladium

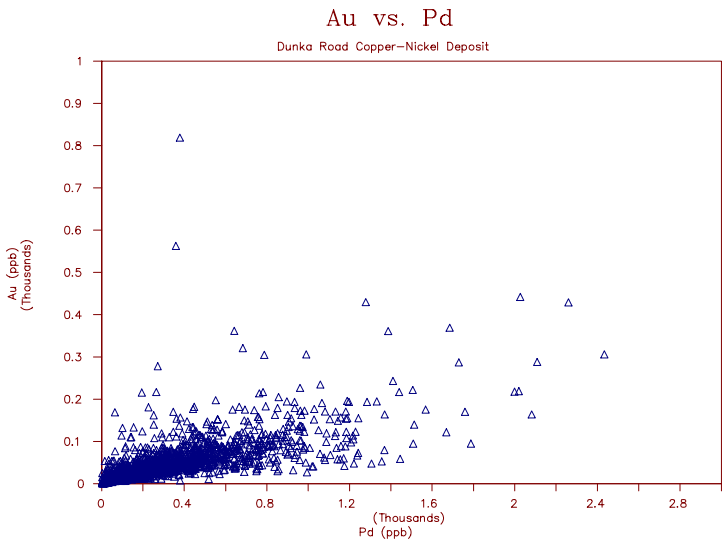

Figure 7. Palladium vs. Gold

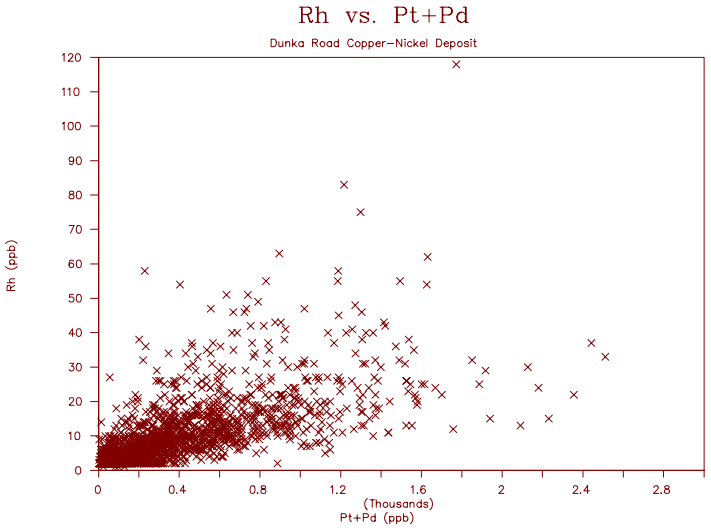

Figure 8. Rhodium vs. Platinum + Palladium

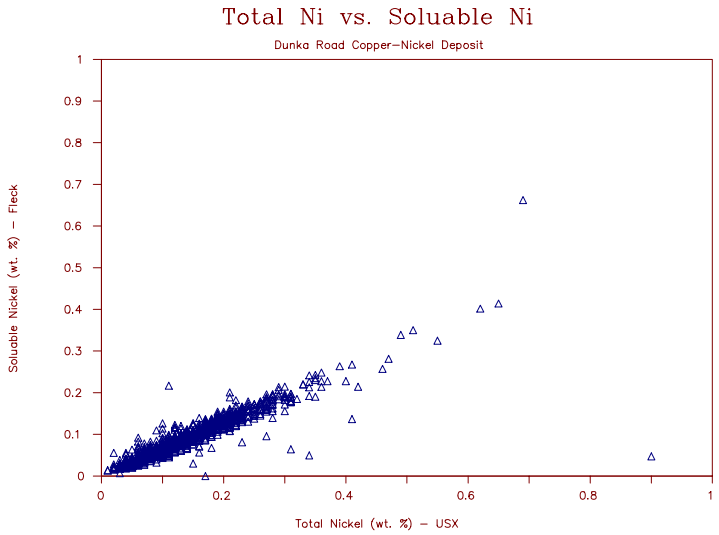

Figure 9. Soluble Nickel vs. Total Nickel

The geochemical assay data reveals some interesting relationships between the PGE content and Cu-Ni mineralization. High Pd values are generally associated with high Cu values. The overall relationship of Cu-Ni ratio is approximately 3:1. As seen in Figures 4-9 and from the correlation coefficients, a few generalizations can be made about the relationship of PGEs and the other elements. The relationship between Pd and Pt is fairly consistent throughout the study area, with a correlation coefficient of 0.741, and a Pd:Pt ratio of 3:1 (Fig. 4). There is also a strong correlation between Pd, Au, and Ag with Cu (Tables 7 and 8; Figs. 5 & 6). Gold is strongly correlated with palladium (Tables 7 and 8; Fig. 7). The correlation of sulfur with Pt, Pd, and Au is poor (not shown; with Pt + Pd 0.182; with Au 2.228). This relationship suggests that the precious metals, particularly Pt, Pd, and Au, are associated with copper-rich sulfide mineralization rather than copper-poor sulfide mineralization.

The Fleck data also contains Rh data. Rhodium is correlated with Pt and Pd. (Tables 7 and 8; Fig. 8). Yet, when correlated separately, there is a closer relationship of Rh with Pd (0.655) than with Pt (0.572).

Since the Dunka Road geochemical data file (Appendix C) contains both USX

values (total Ni, i.e., total acid dissolution) and Fleck values (soluble Ni, i.e., HNO_3 + HCl dissolution), comparison of sulfide (soluble) Ni to total (silicate + soluble) Ni content is possible (Fig. 9). There is a strong correlation coefficient of 0.7802 calculated with 1512 pairs. The calculated slope of total Ni and soluble Ni is 0.7657, with a ratio of total Ni to soluble Ni of 3:2, respectively.

ALTERATION/FRACTURING

Although most rock within the deposit is unaltered, an estimate of the actual percentage of rock affected by alteration is difficult. Still, moderate amounts of alteration are associated with approximately 60 percent of the high grade sulfide zones. It has not yet been determined whether these alteration zones have any relationship with high grade sulfide zones. If there is a relationship then these zones may represent late-stage fluid movement along fractures. Also associated with these zones are varying degrees of fracturing. Most of the high grade zones are moderately fractured. The orientation of fractures within the high grade zones is extremely variable (core angles of 5 to 85 degrees). Alteration is concentrated along the fractures. The alteration occurs as moderate chloritization and weak serpentinization. In many zones, the pyroxenes are uralitized. Varying degrees of uralitization occur as an amorphous, light green and relatively soft replacement. Although difficult to observe in core, minor amounts of microfracturing are also present. The microfracturing is most visible in zones that contain uralite and bleached plagioclase.

PGM CHONDRITE PLOT

Table 1 lists the PGE-Au-Ag-Cu-Ni values for high grade intersections in five drill holes.

Table 1. High grade PGE-Au-Ag and Cu-Ni mineralization at Dunka Road.

DDH #	Footage	Cu	Ni	Pt	Pd	Ir	Os	Rh	Ru	Au	Ag
26010*	115.5-118.5	5.64	0.64	<100	9400	9.0	<10.0	85	<50	2100	15.0
26028	96-113	0.15	0.05	2000	21	3.0	<2.0	4	<10	11	0.4
26060	109-119	0.94	0.17	350	1390	6.0	<2.0	47	20	61	2.9
26098	438-448	0.70	0.12	70	270	1.0	<2.0	7	<10	7	2.1
26128	615-625	0.74	0.15	72	260	1.0	<2.0	9	<10	5	2.5

Note: Cu, Ni in wt. %, Ag in ppm, other elements in ppb. Analyses done by Bondar-Clegg; PGEs+Au by neutron activation, Cu, Ni and Ag by atomic absorption: * Cu, Ni and Ag by assay during an earlier sample run see Morton and Hauck (1987).

Figure 10 illustrates the average chondrite-normalized PGE+Au concentrations in the sulfide fraction (after Naldrett and Duke, 1980) for the values in Table 1. The PGE chondrite plots assume that all the PGEs are magmatic and have not been remobilized.

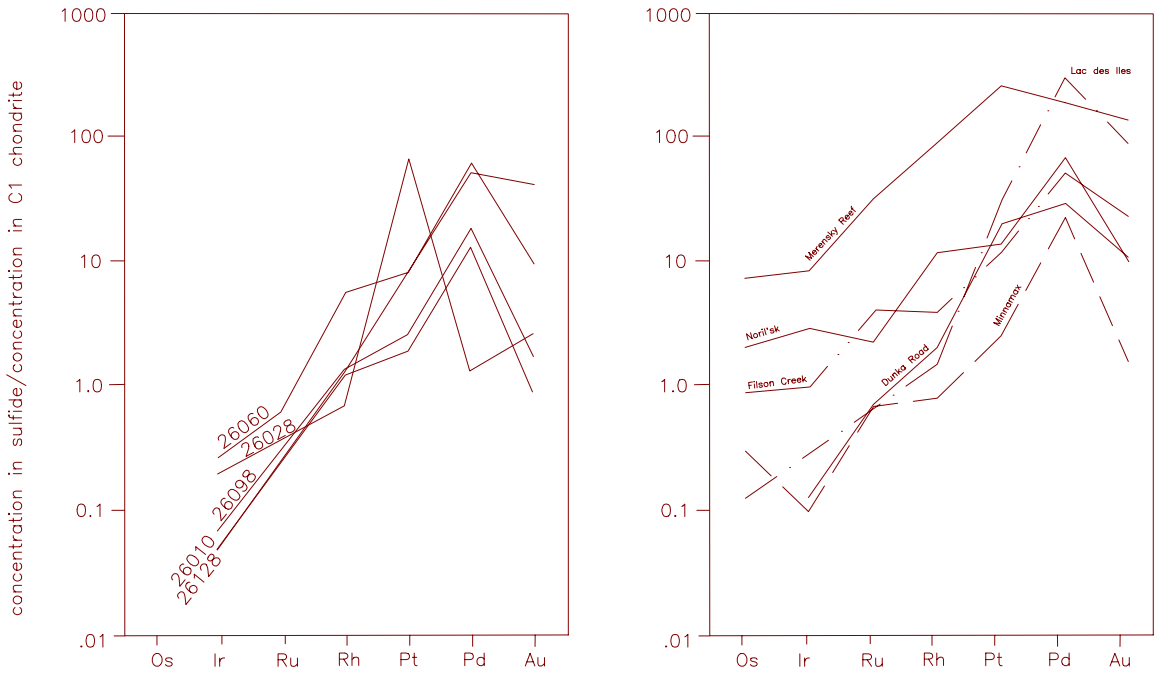

Figure 10. PGE Chrondrite Plots. A (left) - Dunka Road; B (right) - Other PGM deposits with Dunka Road (after Naldrett and Duke,1980 and Sutcliffe, *et al*, 1989; and this study).

As discussed in previous sections, the elemental ratios suggest a hybrid (magmatic-hydrothermal) origin. Figure 10B compares the average PGE chondrite normalized values at Dunka Road to other PGE occurrences at Minnamax and South Filson Creek. The Dunka Road samples are depleted in Os, Ir and Ru compared to the other deposits. The Dunka Road values are closer to the Noril'sk values than the other Duluth Complex deposits. The Dunka Road and South Filson Creek Pd-Au values are similar. Average Pd at the Minnamax/Babbitt deposit compare similarly also, suggesting a common origin.

GEOSTATISTICS

DATA SUMMARY

Drilling Statistics

The Fleck Resources data set is comprised of 86,444 feet of drilling in 84 core holes (Appendices B and C). The shortest hole is 162 feet, the longest hole is 2,647 feet, and the average hole length is 1,029 feet. Figure 11 shows a posting of the 84 collar locations. While there are variations in the drilling pattern, the average distance between collars is approximately 300 feet.

Of the 84 core holes, 72 are recorded as vertical. The 12 reported angle holes dipped between 40 and 60 degrees. All reported borehole orientations are based on collar surveys: there is no record of "down-the-hole" surveys on any of the 84 cores.

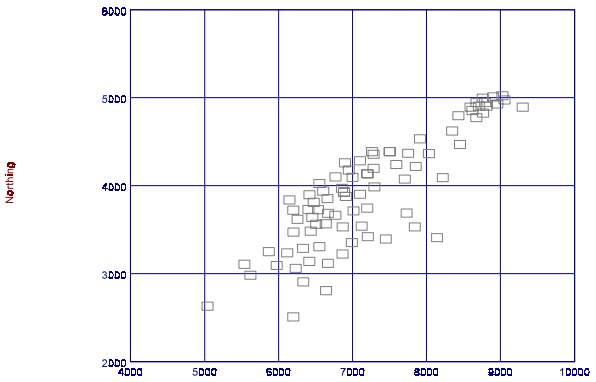

Figure 11. Collar easting locations.

The 84 core holes include 1,890 assays. While the individual assay lengths vary from 1 to 15 feet, the vast majority of the assays are supported by 10 feet of core. The total assayed length is 17,433.2 feet; thus, the average assay length is 9.2 feet.

The "standard assay length" is 10 feet, but the beginning and ending points for assaying were ultimately determined by visual inspection of the core. Visually barren lengths of core were not assayed. On the other hand, numerous exceptional core segments were assayed more than once. Duplicate samples account for 206 out of the total 1,890 assays. The number of assay lengths per hole vary from a minimum of 1 to a maximum of 48; the average number of assay lengths per hole is 22.5.

Summary Statistics

Table 2 presents a suite of summary statistics for all seven assayed elements: Cu, Ni, Ag, Au, Pt, Pd, and Rh. These statistics are based upon all 1,890 assays - duplicate assays are included in the analysis. Furthermore, these statistics do not include any length weighting, so a one foot assay interval is given as much weight as a ten foot assay interval.

Table 2. Summary statistics for the Fleck Resources data set. These statistics are based upon all available assays - duplicates assays were included in the analysis.

	Cu (%)	Ni (%)	Ag (ppm)	Au (ppb)	Pt (ppb)	Pd (ppb)	Rh (ppb)
N used	1890	1890	1890	1890	1890	1890	1643
N missing	0	0	0	0	0	0	247
Mean	0.346	0.085	1.21	49.1	91.1	318.0	10.5
Variance	0.061	0.005	0.78	4465.2	9547.4	150639.2	112.4
Std. Dev.	0.248	0.072	0.89	66.8	97.7	388.1	10.6
Coef. Var.	71.632	84.246	73.24	136.2	107.3	122.1	100.6
Skewness	4.071	17.555	2.50	13.7	2.6	10.2	3.7
Kurtosis	63.024	539.601	23.27	344.3	13.7	243.1	32.1
Minimum	0.001	0.000	0.1	1	1	1	1
25th %tile	0.174	0.050	0.6	18	26	87	3
Median	0.296	0.075	1.0	33	61	218	8
75th %tile	0.470	0.110	1.6	60	122	439	14
Maximum	4.890	2.359	13.3	1926	907	10386	151

Of particular note in Table 2 are the significant differences between the maximums and the 75th percentiles for the seven elements. In all cases, the extreme highs are not supported by the bulk of the assay data.

As a specific example, the highest silver, gold, palladium, and rhodium assays occurred in one three-foot interval of one hole: 115.5 to 118.5 feet in hole number 26010. On either side of this interval the rock is barren (assays were not even taken). Furthermore, an investigation of neighboring holes found no indication of horizontal continuity whatsoever.

A similar example was hole 26043. This hole had one assay interval. This one assay interval is one foot long. Yet, the Ni assay for this one foot assay is almost four times as large as the second largest Ni assay. In an effort to determine the effects of the extreme highs on the summary statistics, a robust version of the summary statistics are presented in Table 3. These statistics were calculated after removing the highest one-half of one percent of the data (10 assay values). A different set of 10 assays were removed for each of the seven elements. By comparing Table 2 and Table 3, an extremely small fraction of the data (one-half of one percent) has a significant impact on the summary statistics.

Table 3. Robust summary statistics for the Fleck Resources data set. These statistics were calculated after removing the highest one-half of one percent of the assay values for each of the seven elements (10 assay values).

	Cu (%)	Ni (%)	Ag (ppm)	Au (ppb)	Pt (ppb)	Pd (ppb)	Rh (ppb)
N used	1880	1880	1880	1881	1880	1880	1635
N missing	10	10	10	9	10	10	255
Mean	0.339	0.083	1.19	46.4	88.0	304.8	10.2
Variance	0.046	0.002	0.63	1771.3	7586.3	82803.6	81.8
Std. Dev.	0.214	0.044	0.79	42.1	87.1	287.8	9.0
Coef. Var.	63.074	53.130	66.87	90.8	98.9	94.4	88.7
Skewness	0.860	0.912	1.02	2.3	1.8	1.5	1.8
Kurtosis	3.388	3.853	3.96	10.5	6.4	5.6	7.0
Minimum	0.001	0.000	0.1	1	1	1	1
25th %tile	0.174	0.050	0.6	18	26	87	3
Median	0.295	0.074	1.0	33	61	218	8
75th %tile	0.467	0.110	1.6	60	121	436	14
Maximum	1.124	0.267	4.5	362	525	1728	55

The reported measures of skewness, the relatively high coefficients of variation, and the initial graphical data analyses, indicate that the distributions of all seven elements are asymmetric, with long positive tails. As is common practice in the statistical analysis of base and precious metals, a logarithmic transformation was applied (David, 1977). The resulting logarithmic summary statistics are presented in Table 4.

Table 4. Logarithmic summary statistics for the Fleck Resources data set. These statistics are based upon all available assays - duplicates assays were included in the analysis.

	Ln(Cu) (%)	Ln(Ni) (%)	Ln(Ag) (ppm)	Ln(Au) (ppb)	Ln(Pt) (ppb)	Ln(Pd) (ppb)	Ln(Rh) (ppb)
N used	1890	1890	1890	1890	1890	1890	1643
N missing	0	0	0	0	0	0	247
Mean	-1.317	-2.637	-0.085	3.491	3.956	5.204	1.971
Variance	0.658	0.369	0.660	0.818	1.414	1.421	0.793
Std. Dev.	0.811	0.607	0.813	0.904	1.189	1.192	0.891
Coef. Var.	61.554	23.029	961.589	25.899	30.056	22.902	45.202
Skewness	-1.394	-0.902	-0.739	-0.195	-0.693	-0.681	0.049
Kurtosis	8.452	10.614	3.548	3.577	3.583	3.405	2.210
Minimum	-7.419	-9.210	-2.303	0.000	0.000	0.000	0.000
25th %tile	-1.744	-2.995	-0.511	2.890	3.258	4.466	1.099
Median	-1.218	-2.594	0.000	3.511	4.111	5.389	2.079
75th %tile	-0.754	-2.203	0.470	4.094	4.804	6.084	2.639
Maximum	1.587	0.858	2.588	7.563	6.810	9.248	5.017

The logarithmic histograms for all seven elements are presented in Figures 12 through 19. These seven figures, in addition to the log-normal probability plots, indicate that the log-normal distribution (David, 1977) is a reasonable model for all seven elements. However, the slight asymmetry in the logarithmic histograms, and the slight curvatures in the log-normal probability plots of Cu, Ni, Ag, Au, Pt, and Pd suggest that a three parameter log-normal model is more appropriate. This observation is further substantiated by the negative skewness of the logarithmic transformations of these six elements. A two parameter (standard) log-normal model is appropriate for Rh.

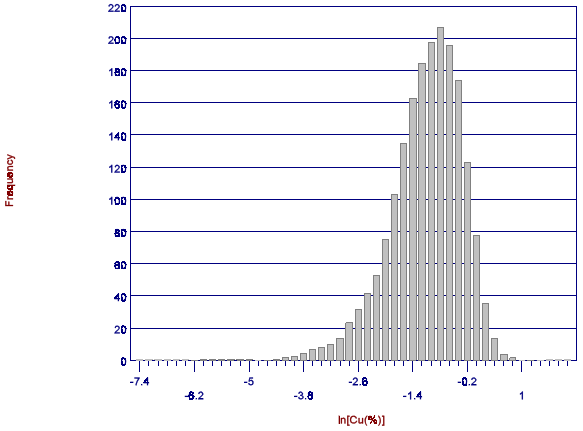

Figure 12. Histogram of ln (Cu wt. %) - Fleck data set.

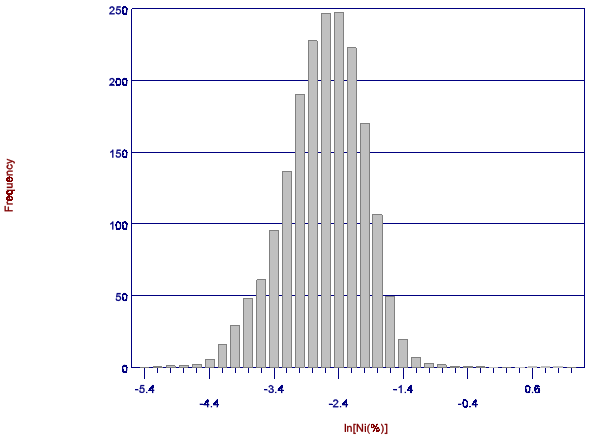

Figure 13. Histogram of ln (Ni wt. %) - Fleck data set.

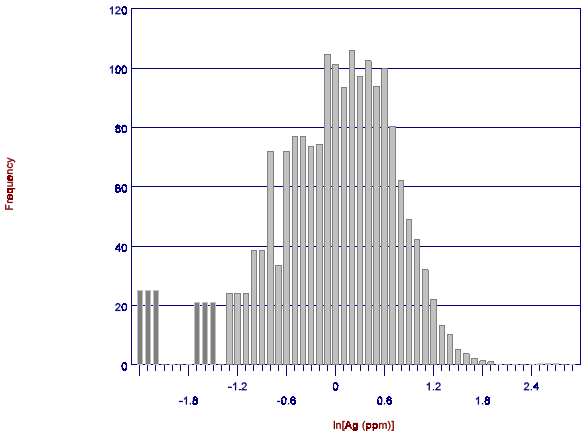

Figure 14. Histogram of ln (ppm Ag) - Fleck data set.

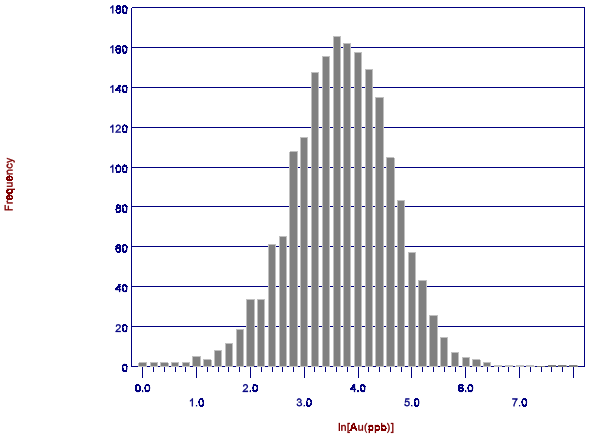

Figure 15. Histogram of ln (ppb Au) - Fleck data set.

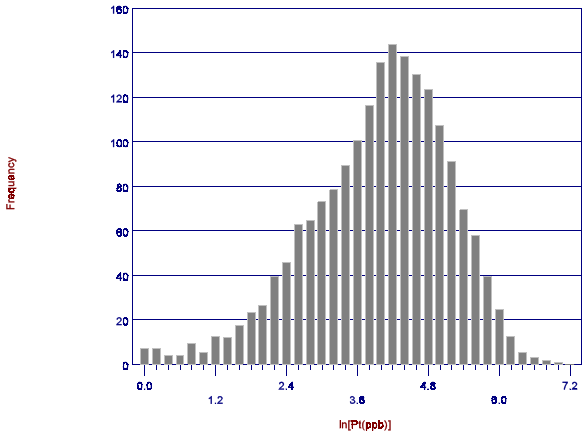

Figure 16. Histogram of ln (ppb Pt) - Fleck data set.

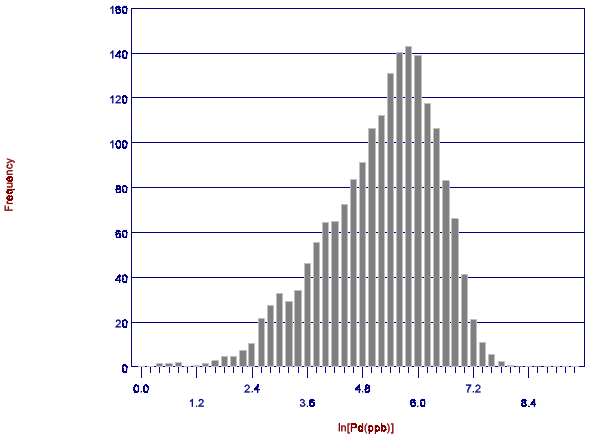

Figure 17. Histogram of ln (ppb Pd) - Fleck data set.

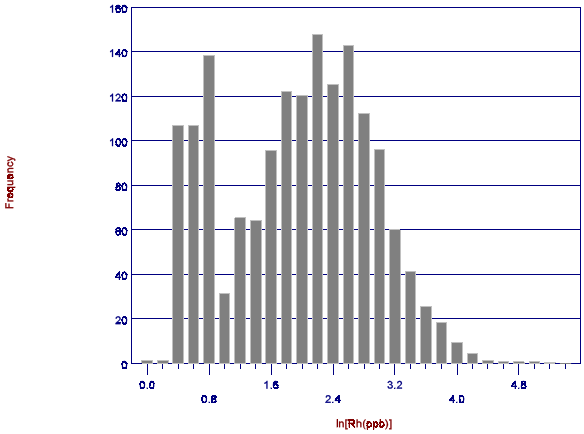

Figure 18. Histogram of ln (ppb Rh) - Fleck data set.

Data Summary for the USX Data Set

Table 5 presents a suite of summary statistics for all four assayed elements: Cu, Ni, S, and Fe. These statistics are based upon all 2,053 assays - duplicate assays were included in the analysis. Furthermore, these statistics do not include any length weighting, so a one foot assay was given the same weight as a ten foot assay interval. The logarithmic summary statistics are presented in Table 6.

Table 5. Summary statistics for the USX data set. These statistics are based upon all available assays - duplicates assays were included in the analysis.

	Cu(%)	Ni(%)	S(%)	Fe(%)
N used	2053	2053	2020	1950
N missing	0	0	33	103
Mean	0.372	0.139	0.945	10.243
Variance	0.072	0.007	1.015	5.747
Std. Dev.	0.269	0.086	1.008	2.397
Coef. Var.	72.152	61.864	106.598	23.406
Skewness	4.442	4.814	8.589	1.866
Kurtosis	75.056	74.694	129.693	14.514
Minimum	0.000	0.010	0.020	0.800
25th %tile	0.180	0.080	0.480	8.740
Median	0.330	0.120	0.765	9.960
75th %tile	0.500	0.180	1.130	11.220
Maximum	5.640	1.790	21.680	36.800

Table 6. Logarithmic summary statistics for the USX data set. These statistics are based upon all available assays - duplicates assays were included in the analysis.

	Ln[Cu]	Ln[Ni]	Ln[S]	Ln[Fe]
N used	2044	2053	2020	1950
N missing	0	0	33	103
Mean	-1.238	-2.131	-0.331	2.302
Variance	0.620	0.325	0.563	0.051
Std. Dev.	0.787	0.570	0.750	0.225
Coef. Var.	63.625	26.733	226.410	9.764
Skewness	-0.936	-0.325	-0.516	-0.510
Kurtosis	4.535	3.528	5.461	12.839
Minimum	-4.605	-4.605	-3.912	-0.223
25th %tile	-1.661	-2.526	-0.734	2.168
Median	-1.109	-2.120	-0.268	2.299
75th %tile	-0.693	-1.715	0.122	2.418
Maximum	1.730	0.582	3.076	3.605

The logarithmic histograms for Cu and Ni are presented in Figures 19 and 20.

These two figures indicate that the log-normal distribution is a reasonable model for the two elements. As with the Fleck Resources data set, slight curvatures in the log-normal probability plots for Cu and Ni suggest that a three parameter log-normal model is more appropriate. This observation is further substantiated by the negative skewness of the logarithmic transformations of these elements.

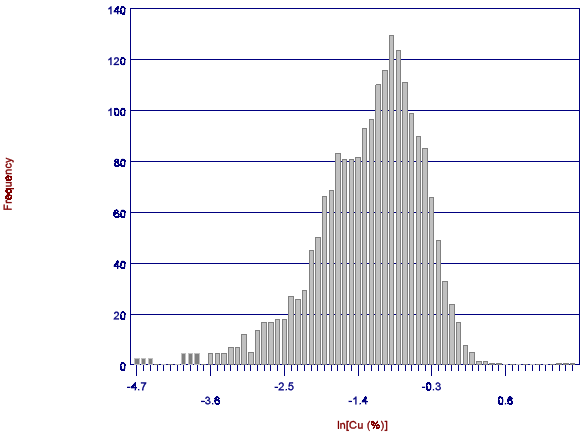

Figure 19. Histogram of ln (Cu wt. %) - USX data set.

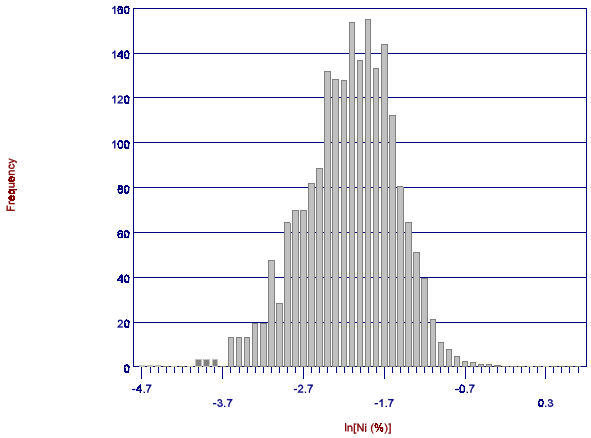

Figure 20. Histogram of ln (Ni wt. %) - USX data set.

The USX data set does not appear to be significantly different from the Fleck Resources data set. The small differences between can be explained by the differences in the sampled materials. The difference in the nickel statistics between the USX and Fleck data sets is the result of analyzing for total nickel versus soluable nickel, respectively. As such, the limited suite of elements included in the USX data set make it unattractive for further statistical analysis at this time.

Inter-Variable Correlations

The inter-variable correlations (Isaaks and Srivastava, 1989) between the seven elements are presented in Table 7. The high correlation between Cu and Ni (88%) indicates that the two metals would be mutually selectable. In a selective mining operation, targeting the ore-grade copper will simultaneously target the ore-grade nickel.

Similarly, the high correlation between Cu and Ag (86%) indicates that a mine plan focusing on copper and nickel would capture most of the ore-grade silver.

Table 7. Inter-variable correlations for the Fleck Resources data set.

[Cu]	1.000						
[Ni]	0.880	1.000					
[Ag]	0.858	0.765	1.000				
[Au]	0.606	0.575	0.611	1.000			
[Pt]	0.601	0.594	0.591	0.666	1.000		
[Pd]	0.733	0.682	0.689	0.686	0.741	1.000	
[Rh]	0.581	0.549	0.544	0.521	0.572	0.655	1.000
	[Cu]	[Ni]	[Ag]	[Au]	[Pt]	[Pd]	[Rh]

Though the correlations between the other four elements are relatively lower (. 65% to 75%), the associations between Au, Pt, Pd, and Rh are significant. Again, these correlations indicate that polymetallic selection of ore zones is potentially practical.

The computed inter-variable correlations for the Fleck Resources data set are verified by the equivalent calculations for the Cu and Ni in the USX data set. These correlations are shown in Table 8.

Table 8. Inter-variable correlations for the USX data set.

[Cu]	1.000			
[Ni]	0.790	1.000		
[S]	0.424	0.510	1.000	
[Fe]	0.225	0.312	0.651	1.000
	[Cu]	[Ni]	[S]	[Fe]

In a polymetallic deposit, the inter-variable correlations can yield useful information for the corroboration of various depositional hypotheses. Specifically, the high correlations are evidence that a single geologic event/process is responsible for the concentration of all seven elements. However, previous studies (Morton and Hauck, 1987, 1989) and this study indicate two geologic events, i.e., primary magmatic and secondary hydrothermal. The high correlation of these values, therefore, suggests the secondary event locally redistributed and concentrated these seven elements.

Observations and Concerns

Of the 86,444 feet of drilled core included in this analysis, only 17,433.2 feet were assayed. The selection of the assay intervals was primarily carried out by visual inspection of the core - zones showing no visible sulfide mineralization were not assayed. In this statistical analysis, all unassayed core are treated as unmineralized. This assumption is necessary to proceed with estimation and inference, yet, it is merely an assumption. It is possible that Ag, Au, Pt, Pd, or Rh could be present at parts-per-million concentrations in the unassayed lengths of core. Statistical analysis of the available data cannot discern the presence of ore-grade metal in vast unsampled zones. Analysis of the unsplit sulfide-bearing zones that had not been sampled shows some zones (under Unit II(a)) had high Pd values but low Cu and Ni values (Tables 9a and 9b). The majority of the unmineralized zones in Unit I for the main host rock, augite troctolite, have background values (limited data set) for Cu, Ni, Pt, Pd and Au of 465 ppm, 232 ppm, 16 ppb, 6 ppb, and 3 ppb, respectively (Severson and Hauck, 1990).

Table 9a. Summary statistics for the unsplit sulfide zones.

	Cu (%)	Ni (%)	Ag (ppm)	Au (ppb)	Pt (ppb)	Pd (ppb)	Rh (ppb)
Mean	0.1726	0.0477	0.8375	37.0	63.8	200.4	8.8
Var	0.0276	0.0019	0.3931	1653.0	11347.1	49715.1	82.3
Std. Dev	0.1663	0.0439	0.6270	40.7	106.5	223.0	9.1
% Coef. Var.	96.3039	92.1335	74.8648	109.9	166.9	111.3	102.7
Skewness	2.2920	4.0739	1.7430	3.36	4.8	1.8	1.6
Kurtosis	10.4381	27.3977	6.0363	19.01	30.4	6.2	5.0
Min	0.0121	0.0070	0.1000	2.0	1.0	5.0	2.0
25th %	0.0629	0.0210	0.4000	13.0	16.0	46.0	2.0
Median	0.1252	0.0380	0.7000	24.0	31.0	111.5	5.0
75th %	0.2052	0.0560	1.0000	41.0	68.0	278.0	13.0
Max	1.0849	0.3730	3.4000	306.0	764.0	1050.0	40.0

Table 9b. Logarithmic summary statistics for the unsplit sulfide zones.

	ln (Cu)	ln (Ni)	ln (Ag)	ln (Au)	ln (Pt)	ln (Pd)	ln (Rh)
Mean	-2.1641	-3.2936	-0.4129	3.2024	3.49	4.668	1.72
Var	0.9050	.4605	0.4783	0.8307	1.35	1.46	0.89
Std. Dev.	.9513	.6786	0.6916	0.9114	1.16	1.21	0.94
% Coef. Var.	43.9593	20.6050	167.4948	28.4603	33.26	25.82	54.74

Skewness	-0.2453	0.3464	-0.0132	-0.0359	-0.1318	-0.2914	0.40
Kurtosis	2.6194	3.4307	3.0332	3.0645	3.54	2.58	1.89
Min	-4.4145	-4.9618	-2.3026	0.6931	0.0	1.61	0.69
25th %	-1.7662	-3.8632	-0.9163	2.5649	2.77	3.83	0.69
Median	-2.0774	-3.2702	-0.3567	3.1781	3.45	4.71	1.61
75th %	-1.5838	-2.8824	0.0000	3.7136	4.22	5.63	2.56
Max	0.0815	-0.9862	1.2238	5.7236	6.63	6.96	3.69

The second significant concern for the data set is the lack of "down-the-hole" surveys. The hole orientations were determined by collar surveys and drilling intentions alone. With an average length exceeding 1,000 feet, hole deviations of hundreds of feet are entirely possible. While the angle holes almost certainly suffer from significant, unknown, hole deviations, the vertical holes are not immune.

Large, unknown, hole deviations can cause two major problems. First, the core may have preferentially aligned itself with relatively weaker sulfide bands. This can result in an a gross overestimation of the thickness and extent of the high grade zones. Second, the spatial statistics and the ultimate spatial interpolation, are sensitive to mislocations of assays. Hole deviations possible in this drilling campaign can easily muddle otherwise clear spatial continuity.

A third concern for the Fleck Resources data set is the lack of a detailed quality assurance analysis for the assays. While there were 206 duplicate assays, these were all taken in an effort to verify extreme or exceptional assays. As such, they are not representative of the bulk of the data. A detailed comparative analysis between the Fleck Resources data set and the USX data set would reduce these concerns, but not eliminate them.

COMPOSITING OF ASSAYS

Base of the Duluth Complex

Severson's (1988) report suggests that the basal contact of the Duluth Complex

with the Virginia Formation (or with the Biwabik Iron Formation) offers a natural datum for the geology at the Dunka Road project.

> "All data collected to date have added immensely to an understanding of the Duluth Complex and its related ore deposits. Contouring of the basal contact of the Complex and top of the Biwabik-Iron Formation has indicated more structure within the Partridge River intrusion than previously recognized. ... Anomalous PGE values occur along a NE-trending fault at Minnamax and thin high-grade copper zones occur along a NW-trending fault at Dunka Road ..."

Plates 4 and 5 illustrate that the higher grade zones follow the rise and fall of the basal contact elevation.

Therefore, the vertical coordinates of the assay values were redefined as the elevation above the basal contact of the Duluth Complex with the Virginia Formation (or the Biwabik Iron-Formation). This redefinition of the geometric coordinate system unfolds the otherwise complex structure. This coordinate transformation is in keeping with the geostatistical mandate to incorporate as much geological insight as possible into the geostatistical analysis (David, 1988; Barnes, 1982; and Dagbert, *et al*, 1984).

Of the 84 core holes in the Fleck Resources data set, 78 intersected the base of the Duluth Complex. A simple planar least squares regression of Easting and Northing versus elevation of the "base of complex" was carried out to quantify the average orientation of the contact surface. The base of the Duluth Complex dips at a little more than 20 degrees, with an average dip direction of approximately S30EE.

The computation of the height above the base for vertical holes that intersected the base was simply a matter of direct subtraction. The estimation of the heights above the base for angle holes and holes that did not intersect the base of the complex were accomplished using universal kriging of the surface from the neighboring data (Davis and David, 1978).

Vertical Compositing

Assays were composited into 25 foot intervals starting at the base of the Duluth Complex. Numerical compositing was necessary to equalize the support (effective assay interval length) of every sample value, and to allow meaningful inference of the spatial correlation structure. The specific choice of 25 feet was motivated by historical precedence, i.e., what is done at existing mines in North America.

During compositing, duplicate samples were averaged. Any intervals of core without assays were treated as barren. The compositing process thus generated many 25 foot intervals with an assigned grade of zero.

Composite Summary Statistics

There are 3,131 composites in the composite data base generated using the Fleck Resources data set. Approximately three quarters of these composites are barren. Table 10 shows the summary statistics for all of the composites, including the approximately 2,300 barren intervals. Not surprisingly, the overall average is severely depressed when compared to the mean of the mineralized assays. Since the core holes were drilled roughly on regular grid, the statistics in Table 10 can be interpreted as the overall statistics for the prospect. Since these statistics do not incorporate any sense of mining selectivity, they cannot be interpreted, in any sense, as describing the "ore reserves."

Table 10. Summary statistics for the Composite data set. These statistics are based upon all of the composites, including the barren intervals.

	Cu	Ni	Ag	Au	Pt	Pd	Rh

	(%)	(%)	(ppm)	(ppb)	(ppb)	(ppb)	(ppb)
N used	3131	3131	3131	3131	3131	3131	3131
N missing	0	0	0	0	0	0	0
Mean	0.078	0.019	0.27	10.9	20.7	71.9	2.0
Variance	0.032	0.002	0.41	820.6	2990.9	38085.7	29.1
Std. Dev.	0.180	0.041	0.64	28.6	54.7	195.2	5.4
Coef. Var.	230.384	218.081	234.31	263.1	264.7	271.6	265.1
Skewness	3.294	2.738	3.49	5.1	4.3	5.0	4.1
Kurtosis	18.445	11.966	20.71	48.1	30.5	48.9	24.6
Minimum	0.000	0.000	0.0	0	0	0	0
25th %tile	0.000	0.000	0.0	0	0	0	0
Median	0.000	0.000	0.0	0	0	0	0
75th %tile	0.022	0.010	0.1	3	3	11	0
Maximum	2.170	0.340	7.8	502	736	3576	51

Table 11 shows the summary statistics for the mineralized composites; the effects from all of the barren intervals have been eliminated. Comparing Table 11 with Table 2 and Table 3, the effects of compositing can be discerned. The extremes for the composited data are noticeably less, as are the means. The standard deviations, however, are not radically changed.

Table 11. Summary statistics for the mineralized intervals in the Composite data set. These statistics do not include the barren intervals.

	Cu (%)	Ni (%)	Ag (ppm)	Au (ppb)	Pt (ppb)	Pd (ppb)	Rh (ppb)
N used	815	797	802	817	815	819	746
N missing	2316	2334	2329	2314	2316	2312	2385
Mean	0.300	0.074	1.06	41.7	79.4	274.7	8.5
Variance	0.058	0.003	0.75	1859.7	6833.5	89947.0	66.7
Std. Dev.	0.241	0.051	0.86	43.1	82.7	299.9	8.2
Coef. Var.	80.140	68.219	81.41	103.4	104.1	109.2	95.6
Skewness	1.849	1.370	2.05	3.2	2.3	2.9	2.1
Kurtosis	9.552	6.000	10.68	23.4	12.5	22.6	8.8
Minimum	0.010	0.010	0.1	1	1	1	1
25th %tile	0.130	0.040	0.5	14	19	62	3
Median	0.240	0.060	0.8	29	56	179	6
75th %tile	0.420	0.100	1.4	53	106	381	12
Maximum	2.170	0.340	7.8	502	736	3576	51

As with the raw assays, the reported measures of skewness, the relatively high coefficients of variation, and the initial graphical data analyses, indicate that the

distributions of all seven elements are asymmetric, with long positive tails. As such, a logarithmic transformation is applied. The resulting logarithmic summary statistics are presented in Table 12. By the very nature of the logarithm, the statistics in Table 12 do not include the barren intervals.

Table 12. Logarithmic summary statistics for the mineralized intervals of the Composite data set. By the very nature of the logarithm, these statistics do not include the barren intervals.

	Ln(Cu) (%)	Ln(Ni) (%)	Ln(Ag) (ppm)	Ln(Au) (ppb)	Ln(Pt) (ppb)	Ln(Pd) (ppb)	Ln(Rh) (ppb)
N used	815	797	802	817	815	819	746
N missing	2316	2334	2329	2314	2316	2312	2385
Mean	-1.561	-2.852	-0.275	3.258	3.768	4.963	1.726
Variance	0.917	0.593	0.783	1.136	1.626	1.789	0.920
Std. Dev.	0.957	0.770	0.885	1.066	1.275	1.338	0.959
Coef. Var.	61.322	27.001	321.894	32.706	33.847	26.953	55.577
Skewness	-0.887	-0.588	-0.538	-0.565	-0.697	-0.774	-0.168
Kurtosis	3.861	2.914	2.908	3.215	3.034	3.442	2.317
Minimum	-4.605	-4.605	-2.303	0.000	0.000	0.000	0.000
25th %tile	-2.040	-3.219	-0.693	2.639	2.944	4.127	1.099
Median	-1.427	-2.813	-0.223	3.367	4.025	5.187	1.792
75th %tile	-0.868	-2.303	0.336	3.970	4.666	5.942	2.485
Maximum	0.775	-1.079	2.054	6.219	6.601	8.182	3.932

The logarithmic histograms for all seven elements are presented in Figures 21 through 27. Using a similar analysis to that of the raw assays, these seven figures indicated that the log-normal distribution is a reasonable model for all seven elements. In particular, a three parameter log-normal model appears to be more appropriate for the seven elements. This observation is further substantiated by the negative skewness of the logarithmic transformations of these six elements.

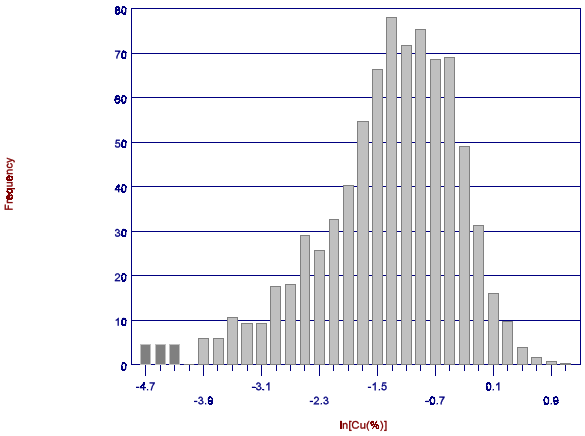

Figure 21. Histogram of ln (composite Cu).

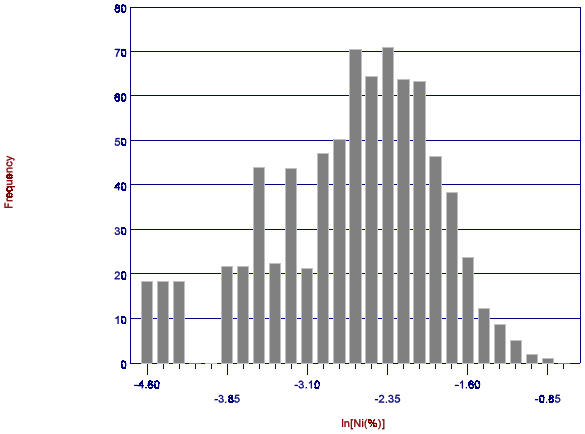

Figure 22. Histogram of ln (composite Ni).

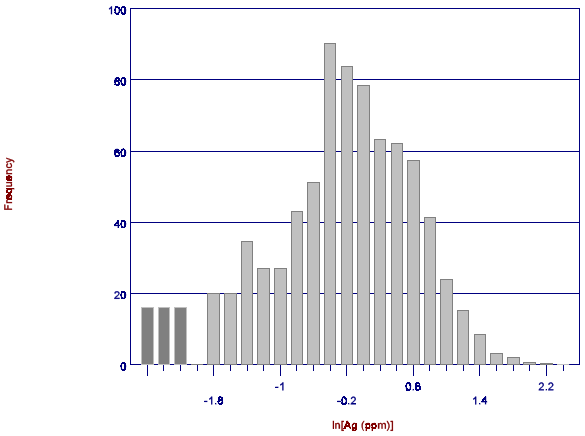

Figure 23. Histogram of ln (composite Ag).

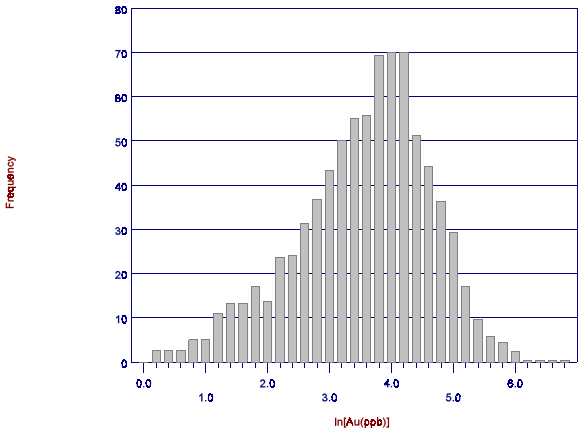

Figure 24. Histogram of ln (composite Au).

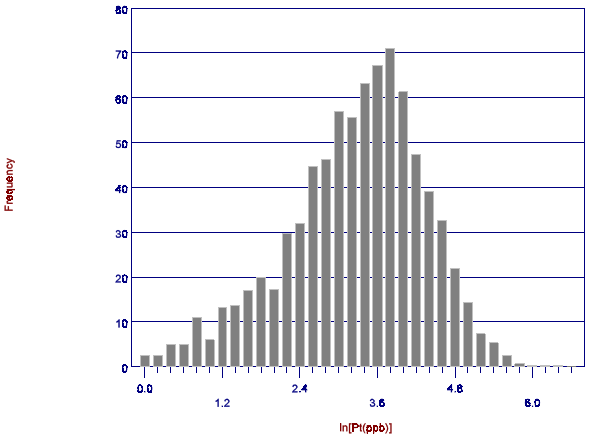

Figure 25. Histogram of ln (composite Pt).

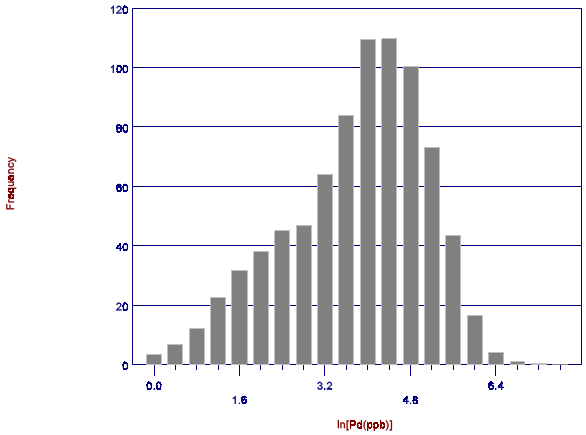

Figure 26. Histogram of ln (composite Pd).

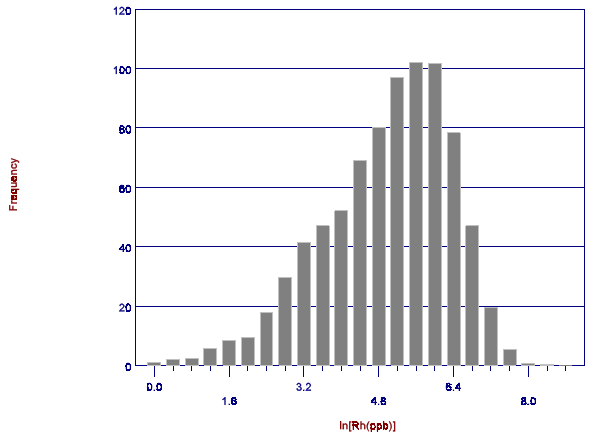

Figure 27. Histogram of ln (composite Rh).

GROSS ECONOMIC AUXILIARY VARIABLE

Creating the Auxiliary Variable

Due to the time constraints on this analysis, a detailed study of each individual element is not possible. Rather, an auxiliary variable combining all seven elements into one gross economic indicator is generated and investigated. This new variable is the sum of the seven metal grades times their respective market prices. The result is expressed in dollars per ton. This does not incorporate any reduction in value due to metallurgical recovery, and this new variable does not include the cost associated with the extraction, processing, or sales of a product. Nonetheless, a market price weighting of the individual elements offers a simple, easy to understand, means of data analysis.

The market prices used were taken from the Engineering and Mining Journal (1989):

Cu	$1.33 / lb
Ni	$5.95 / lb
Ag	$5.16 / tr oz
Au	$362.00 / tr oz
Pt	$485.00 / tr oz
Pd	$136.00 / tr oz
Rh	$1,260.00 / tr oz

The resulting auxiliary variable is defined by the following equation:

$$\$/\text{ton} = 26.6\ (\%\ \text{Cu}) + 119.0\ (\%\ \text{Ni}) + 0.1505\ (\text{ppm Ag}) + 0.01056\ (\text{ppb Au}) + 0.01415\ (\text{ppb Pt}) + 0.003967\ (\text{ppb Pd}) + 0.03675\ (\text{ppb Rh})$$

Summary Statistics for the Auxiliary Variable

There are 3,131 composites in the composite data base. The auxiliary variables

for 819 of these composites have non-zero economic value. Table 13 shows a suite of summary statistics for the auxiliary variable. The first column includes all of the composites, the logarithmic summary statistics, and the last column is the summary statistics of the mineralized intervals when the composite grades are calculated without the highest one-half of one percent of the raw assay values.

Table 13. Summary statistics for the gross economic auxiliary variable. [all] includes all of the composites. [>0] includes only the mineralized intervals. Ln($/t) is the logarithmic summary statistics. [cut] includes only the mineralized intervals, and it excludes the highest one-half of one percent of the raw assays as well.

	$/t [all]	$/t [>0]	Ln($/t)	$/t [cut]
N used	3131	819	819	819
N missing	0	2312	2312	2312
Mean	5.15	19.66	2.619	19.27
Variance	132.59	221.45	1.054	204.19
Std. Dev.	11.52	14.88	1.027	14.29
Coef. Var.	223.82	75.71	39.201	74.12
Skewness	2.97	1.52	-1.689	1.23
Kurtosis	14.30	7.04	8.372	4.98
Minimum	0.00	0.02	-3.817	0.02
25th %tile	0.00	8.77	2.172	8.61
Median	0.00	16.36	2.795	16.15
75th %tile	2.12	27.04	3.297	26.74
Maximum	119.51	119.51	4.783	91.69

Not surprisingly, the overall average is severely depressed when compared to the mean of the mineralized intervals. The potential economic significance of the highest one-half of one percent of the assays is shown by a comparison of the second and fourth columns in Table 13. The difference is noticeable, but not significant in this rough analysis.

Figure 28 shows the histogram for the gross economic auxiliary variable. This figure includes all of the composites. As can be seen, the barren composites dominate the histogram. Figure 29 shows the histogram for the gross economic auxiliary variable

without the barren composites. Only one out of 3,131 composites is above $100 per ton (excluding recovery losses).

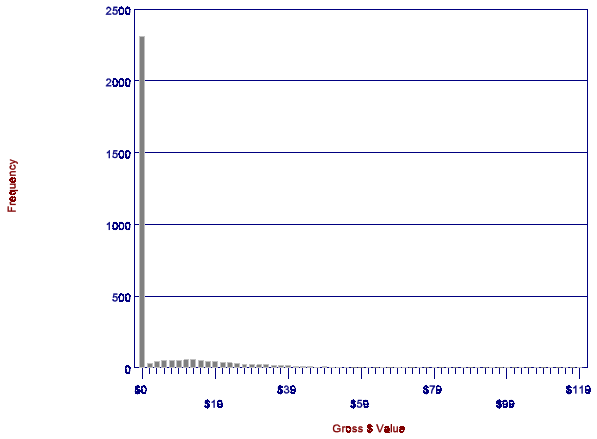

Figure 28. Histogram of the gross auxiliary variable ($/ton).

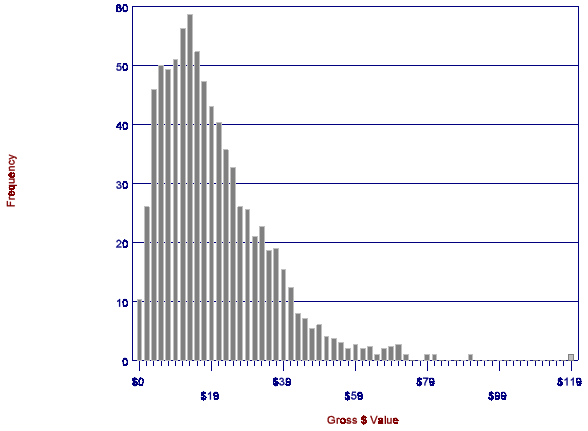

Figure 29. Histogram of gross economic auxiliary variable ($/ton) with non-barren composites.

Unlike the raw assays and unlike the composite assays, the economic auxiliary variable is not particularly well modelled by a log-normal distribution; there are an excessive number of low values.

Value as a Function of Height

As discussed previously, the vertical coordinate for the composite values is given as the height above the base of the Duluth Complex. This coordinate transformation was motivated by geologic reasoning, and it is supported by the following economic presentation.

Figure 30 shows a scatter plot of the mean auxiliary variable versus the height above the base of the complex. This plot shows an unequivocal pattern: the zone between 100 feet above the base up to 400 feet above the base captures the economically interesting mineralization. There is one significant exception to this observation. Adjacent holes 26121 and 26056 have a wide higher-grade band at 1700-1800 ft. and 1300-1450 ft., respectively. This plot further verifies the equivalent observation made from the geologic cross-sections (Plates 4 and 5).

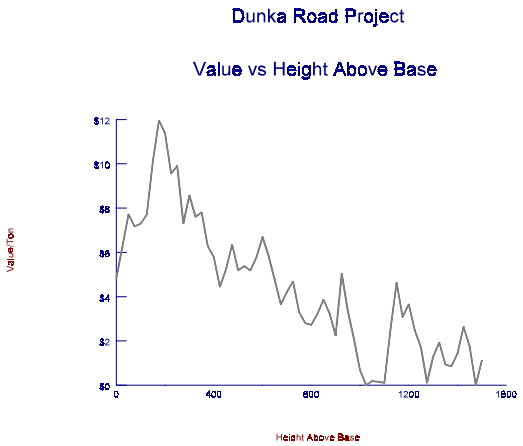

Figure 30. Scatter plot of the average auxiliary variable vs. height above the base of the Duluth Complex.

Ore Reserves

Using the September 1989 metal prices, there are no **ore reserves** in the volume of rock under study in this report. There is but one, spatially unsupported, composite with a gross value in excess of $100 per ton (assuming 100% recovery of all seven

minerals). Given the depth of the mineralized rock, higher grade mineralization would be required to generate profitable ore reserves.

The one, spatially unsupported, composite is again associated with the 3 ft. interval in drill hole 26010. This drill hole (DDH) is one of 12 angle holes drilled in the deposit and the only drill hole to intersect high grade mineralization. As Morton and Hauck (1989) have shown, this intersection is related to secondary or late-stage mineralization. Similarly, in an adjacent drill hole 26028, Morton and Hauck (1989) show a 17 ft. intersection of faulted, highly altered gabbro with an anomalous (chip sampled) Pt assay of 2800 ppb (reassay showed no anomalous Pt). However, the secondary mineralization is related to late-stage faulting (Kuhns, *et al*, 1990) at South Filson Creek. If the high grade intersection in DDH 26010 represents or is related to a steeply dipping, mineralized fault zone, then the vertical holes drilled at Dunka Road would not adequately define this or other potential high grade zones. Consequently, the statistics in this study represent the primary or "laterally" continuous/discontinuous disseminated mineralization and do not address the potential of mineralized high angle fault zones.

SPATIAL STATISTICS AND GEOLOGIC CONTINUITY

Indicator Variograms

Figure 31 shows the three dimensional, omni-directional, indicator semi-variogram for the presence and absence of mineralization. The indicator variable is defined as being a "1" if a composite is barren, and "0" if it is not

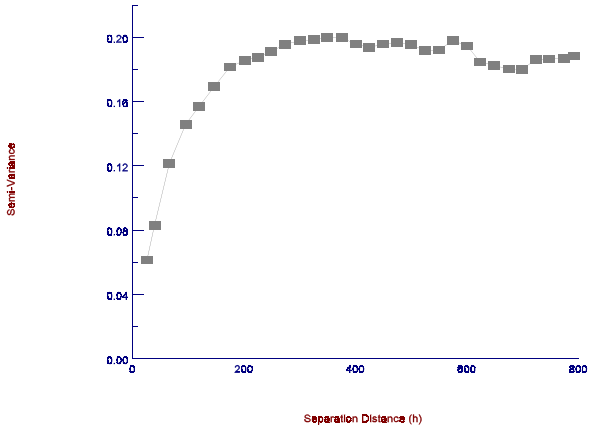

Figure 31. Omni-directional, indicator variogram showing the spatial continuity of the mineralization (includes only high grade composites).

barren (partially mineralized). Thus, the indicator variogram is a reflection of the continuity of mineralization. This figure presents an easily interpreted spatial correlation structure. The sill is approximately 0.18, which is in full agreement with theory's prediction of (0.75 * 0.25) for a 75th percentile indicator. The nugget effect is remarkably small; certainly less than five percent of the sill. The range of the variogram is approximately 400 feet.

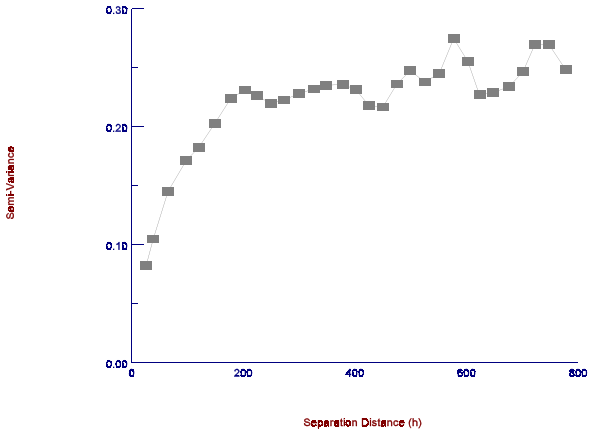

Figure 32. Omni-directional variogram showing the spatial continuity of the mineralization (includes only high grade composites).

Figure 32 presents the indicator semi-variogram for the previously identified high-grade zone; only assays taken between 100 and 400 feet above the base of the complex are included in this figure. Figure 32 shows an equivalent variogram to that given in Figure 31.

Variograms of the Auxiliary Variable

Figure 33 presents the three dimensional, omni-directional variogram for the gross economic auxiliary variable. This plot includes all of the barren composites. Little large scale continuity is discernable.

Figure 34 presents the equivalent omni-directional variogram for the previously identified high-grade zone; only assays taken between 100 and 400 feet

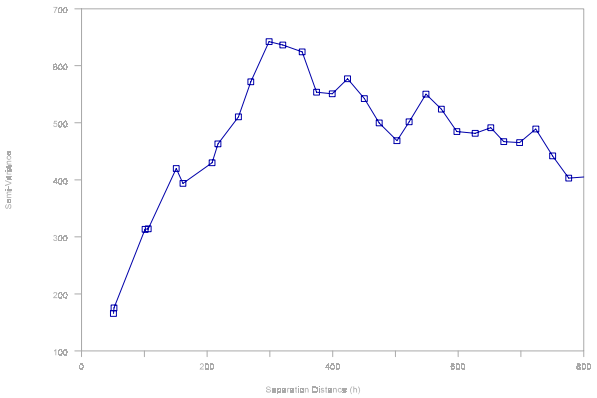

Figure 33. Omni-directional variogram showing the spatial continuity of the gross economic auxiliary variable ($/ton-includes all composites 100-400 ft. above base).

above the base of the complex are included in this figure. (Note the difference in the scaling of the horizontal axis between Figures 33 and 34.) The apparent variogram range is approximately 200 feet, and the apparent variogram nugget effect is, again, remarkably small. The spatial correlation structure shown in Figure 34 is corroborated by Figure 35. This is the variogram of the square-root transformation applied to assays in the high-grade zone.

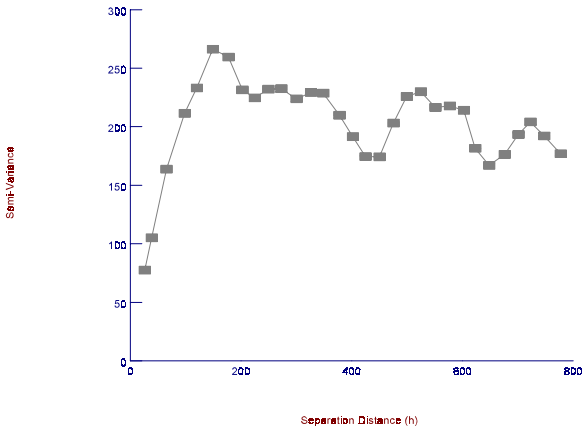

Figure 34. Omni-directional variogram of the gross economic auxiliary variable ($/ton - includes only high grade composites 100-400 ft. above base).

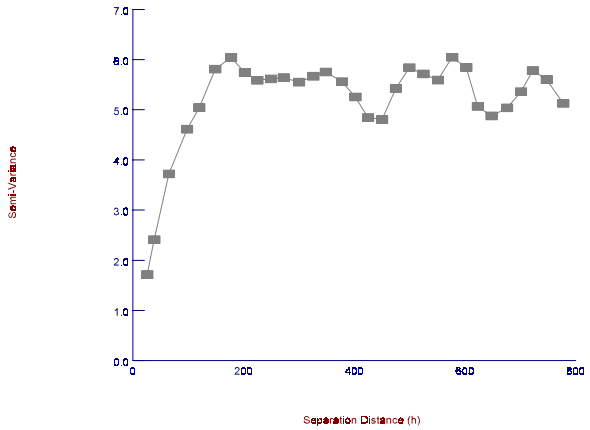

Figure 35. Omni-directional variogram of the gross economic variable sq. root transformation of high grade composites 100-400 ft. above the base.

Geology Revisited

Though additional lithologic information and expert interpretation is available, the base of the Duluth Complex is the only stratigraphic variable incorporated into this analysis. It is conjectured that the development of a more complex, and thus more complete, non-linear coordinate system satisfying all of the known geologic features, would further enhance the spatial analysis. Specifically, all of the identified faults (DDH 26010, 26028, etc.) and folds would have to be incorporated into the coordinate system prior to the generation of a geologic block model, i.e., kriging. However, sufficient angle drilling is not available to adequately assess this model.

SUMMARY

In this report, 1,890 assays from 86,444 feet of drilling, in 84 core holes, are geostatistically investigated to characterize the Dunka Road mineral prospect. The statistical analysis includes seven elements: Cu, Ni, Ag, Au, Pt, Pd, and Rh. While individual assay lengths average approximately 10 feet, a 25 foot composite is used throughout the analysis. During compositing, all unassayed intervals are considered barren. This analysis yields four main conclusions.

First, the base of the Duluth Complex is a critical datum in this mineral prospect. Virtually all of the higher grade rock is contained between 100 and 400 feet above the base of the complex. Though the base of the complex intersects the surface on the north edge of the project, it dips to the SE at approximately 20E. Therefore, most of the potentially interesting mineralization is deeper (greater than 500 feet) southeast of the surface footwall contact.

Second, the marginal distributions for all seven elements can be adequately modelled as log-normal distributions. Furthermore, the inter-variable correlations

between elements are high, indicating that polymetallic mining selectivity is physically possible. The high inter-variable correlation supports local redistribution/concentration of primary mineralization by secondary hydrothermal processes.

Third, the available drilling is sufficient to identify and characterize the spatial correlation structure for the disseminated mineralization. Unambiguous variograms are generated, showing the range of geologic influence to be about 400 feet. No significant vertical to horizontal anisotropy is identified. However, lack of sufficient angle drill holes to evaluate mineralized, higher grade, steeply dipping zones is lacking.

Fourth, given the available drilling, no economic ore reserves are found at the Dunka Road site. Furthermore, given the current horizontal sample spacing, and the identified correlation length, there is little chance that further vertical in-fill drilling will discover any significant quantity of ore within the volume of rock investigated. However, additional angle drilling is required to evaluate the potential of high grade, steeply dipping, mineralized zones.

A more complete, and thus more complex, geostatistical analysis incorporating all of the known geology can then be carried out after additional angle drilling. The results of such a study would be a better model (better in the sense of more accurate local predictions). At the current market prices using the available drilling, the grade of the Dunka Road mineral prospect is insufficient to justify exploitation. It is possible that additional angle drilling may alter this conclusion.

CONCLUSIONS

The geologic study area described represents approximately one fourth the total area of the Dunka Road Cu-Ni mineral deposit. Although Dunka Road represents only a small fraction of the entire Duluth Complex, the knowledge gained by this study should prove useful in understanding and exploring for other Cu-Ni-PGE-Au-Ag occurrences within the Duluth Complex. The rock units delineated by Severson (1988) and Severson and Hauck (1990) are useful in constructing a detailed understanding of the igneous stratigraphy in the Dunka Road area. By subdividing individual rock units, a new set of ore controls, e.g., the ultramafic subunits as redox barriers, are defined that are useful for understanding the PGE and Cu-Ni mineralization.

Generally, each rock unit is characterized by a dominant rock type. However, due to the complexity in each unit and the small amount of rock represented by core, rock types often vary from hole to hole, as in Unit I, due to slight lateral changes in the modal percentage of olivine, pyroxene or plagioclase. Correlation of the ultramafic subunits laterally throughout the area provides an internal structure for each major rock unit that can be used for correlation between drill holes.

Most Cu-Ni mineralization within the area of the study is confined to Unit I and may be vertically limited by the basal ultramafic subunit of Unit II. This `basal zone' type occurrence of sulfides is characteristic of mineralization present within the area of study. However, because most drill holes are collared in Units II and III, sulfides occurring as `cloud zone' type mineralization may be present in Units IV through VIII, and will show up in the deeper drilled holes of Dunka Road.

Changes in the relative percentage of chalcopyrite and pyrrhotite is related to the

distance from hornfels inclusions and/or the basal contact. There is a definite increase in the pyrrhotite to chalcopyrite ratio toward the contact of hornfels inclusions and with the basal contact of the Virginia Formation. Also, high grade zones of mineralization are: 1) internally controlled by and related to specific ultramafic layers within Unit I; and 2) related to possible steeply dipping fault zones or fracture systems as observed in DDH 26010. A preliminary hypothesis is that the PGE-Au-Ag mineralization is directly related to faulting and related fracturing.

The ultramafic subunits may have acted as redox barriers to migrating Cu-PGE-enriched fluids. Fracturing of the troctolites and ultramafic subunits prior to the secondary mineralization provided the pathways for the migrating fluids. The alteration assemblage, secondary sulfide mineralization and fracturing are similar to the mineralization sequence at the South Filson Creek Cu-Ni deposit (Kuhns, *et al*, 1990). Kuhns, *et al* (1990) describe redox boundaries as important to precipitating secondary mineralization. However, the fracturing and alteration preceded secondary mineralization. This same process occurs at Dunka Road as well. A sufficient number of vertical drill holes are available to assess the economic potential of the basal disseminated sulfide mineralization. Geostatistical analyses of these assay data, given the available drill holes, suggest that there are no economic ore reserves in the disseminated mineralization at Dunka Road. However, insufficient angle drilling has been done to assess the economic impact that high grade, e.g., DDH 26010, steeply dipping, fault/fracture zones with semi-massive to massive sulfide mineralization may have on the economic viability of the Dunka Road deposit.

BENEFITS

1. The upper limit of sulfide mineralization is defined by the base of subunit II(a).

2. The ultramafic subunits in Unit I may be important controls on sulfide mineralization.

3. Ultramafic subunits are regional in extent and can be identifiable horizons for exploration drilling and/or mining.

4. PGE-Au-Ag mineralization occurs both laterally and vertically over significant thicknesses and may be an important economic contribution to the economic value of the deposit.

5. Additional angle hole drilling is necessary to assess the potential and impact of high grade, steeply dipping, semi-massive to massive sulfides on the economic viability of the Dunka Road deposit.

REFERENCES

Andrews, M.S., and Ripley, E.M., 1989, Mass transfer and sulfur fixation in the contact aureole of the Duluth Complex, Dunka Road Cu-Ni Deposit, Minnesota: Canadian Mineralogist, v. 27, pp. 293-310.

Barnes, T. E., 1981, Orebody modelling: the transformation of coordinate systems to model continuity at Mount Emmons: Proc. 17th APCOM, AIME, New York, pp. 765-770.

Bonnichsen, B., 1972, Southern part of the Duluth Complex: *in* Sims, P.K., and Morey, G.B., eds., Geology of Minnesota: A Centennial Volume: Minnesota Geological Survey, pp. 361-387.

Dagbert, M., Crozel, D., and Desbarats, A., 1984, Computing variograms in folded strata controlled deposits: *in* Verly, G., David, M., Journel, A., and Marachel, A., eds., Geostatistics for natural resource characterization; Dordrecht, Holland, D. Reidel Pub. Co., pp. 70-90.

David, M., 1977, Geostatistical ore reserve estimation: New York, Elsevier Scientific Pub. Co., pp. 11.

David, M., 1988, Handbook of applied advanced geostatistical ore reserve estimation: New York, Elsevier Scientific Pub. Co., pp. 60-69.

Davidson, D.M., 1972, Eastern part of the Duluth Complex: *in* Sims, P.K., and Morey, G.B., eds., Geology of Minnesota: A Centennial Volume: Minnesota Geological Survey, pp. 354-360.

Davis, M., and David, M., 1978, Automatic kriging and contouring in the presence of trends (universal kriging made simple): J. Can. Petrol, Tech., v. 17, No. 1., pp. 49-68.

Engineering and Mining Journal, 1989, v. 190, no. 9, pp. 21.

Foose, M.P., and Weiblen, P.W., 1986, The physical and chemical setting and textural and compositional characteristics of sulfide ores from the South Kawishiwi Intrusion, Duluth Complex, Minnesota, USA: *in* 27th Int. Geol. Congress (Moscow), Special Copper Symposium, Springer-Verlag, New York, pp. 8-24.

Isaak, E. H., and Srivastava, R. M., 1989, An introduction to applied geostatistics: New York, Oxford Univ. Press, pp. 30.

Kuhns, M.J.P., Hauck, S.A., and Barnes, R.J., 1990, Origin and occurrence of PGMs, Au and Ag in the South Filson Creek Cu-Ni Mineral Deposit, Lake County, Minnesota: Natural Resources Research Institute, Technical Report, NRRI/GMIN-TR-89-15, Duluth, Minnesota, 59 pp.

Listerud, W. H., and Meineke, D. G., 1977, Mineral resources of a portion of the Duluth Complex and adjacent rocks in St. Louis and Lake Counties, northeastern Minnesota: Minn. Dept. Nat. Resources, Div. of Minerals, Report 93, 49 pp.

Morey, G. B., and Cooper, P. W., 1977, Bedrock geology of the Hoyt Lakes-Kawishiwi area, St. Louis and Lake Counties, northeastern Minnesota: Minn. Geol. Survey, open-file map, 1:48,000.

Morton, P., and Hauck, S. A., 1987, PGE, Au and Ag contents of Cu-Ni sulfides found at the base of the Duluth Complex, northeastern Minnesota: Natural Resources Research Institute, Technical Report NRRI/GMIN-TR-87-04, 85 pp.

Morton, P., and Hauck, S. A., 1989, Precious metals in the copper-nickel deposits of the Duluth Complex: Minn. Geol. Survey, Inf. Circ. 30, pp. 47-48.

Naldrett, A. J., and Duke, J. M., 1980, Platinum metals in magmatic sulfide ores: Science, v. 208, no. 4451, pp. 1417-1424.

Phinney, W.C., 1972, Duluth Complex, history and nomenclature: *in* Sims, P.K., and Morey, G.B., eds., Geology of Minnesota: A Centennial Volume: Minnesota Geol. Survey, pp. 333-334.

Ripley, E.M., 1981, Sulfur isotopic studies of the Dunka Road Cu-Ni deposit, Duluth Complex, Minnesota: Econ. Geol., v. 76, pp. 610-620.

Ripley, E.M., and Al-Jassar, T.J., 1987, Sulfur and oxygen isotope studies of melt-country rock interaction, Babbitt Cu-Ni deposit, Duluth Complex, Minnesota: Econ. Geol., v. 82, pp. 87-107.

Severson, M.J., 1988, Geology and structure of a portion of the Partridge River Intrusion, northeastern Minnesota: Natural Resources Research Institute, Technical Report, NRRI/GMIN-TR-88-08, Duluth, Minnesota, 78 pp.

Severson, M.J., and Hauck, S.A., 1990, Geology, geochemistry, and stratigraphy of a portion of the Partridge River Intrusion, northeastern Minnesota: Natural Resources Research Institute, Technical Report, NRRI/GMIN-TR-89-11, Duluth, Minnesota, 240 pp.

Sutcliffe, R. H., Sweeny, J. M., and Edgar, A. D., 1989, The Lac des Iles Complex, Ontario: petrology and platinum-group-elements mineralization in an Archean mafic intrusion: Can. Jour. Earth Sci., v. 26, pp. 1408-1427.

Watowich, S. N., Malcolm, J. B., and Parker, P.D., 1981, A review of the Duluth Gabbro Complex of Minnesota as a domestic source of critical and strategic metals: SME-AIME Fall Meeting, Denver, Colorado, 9 pp.

Weiblen, P.W., and Morey, G.B., 1980, A summary of the stratigraphy, petrology and structure of the Duluth Complex: American Journal of Sci., v. 280, pp. 88-133.

APPENDIX A

Detailed Structural and Thickness Data for Drill Holes

DRILL HOLE #	COLLAR ELEV. (FT.)	HOLE ANGLE (DEG.)	T.D. (FT.)	BASE OF COMPLEX (FT.)	ELEV (FT.)	TOP POKEGAMA (FT.)	ELEV (FT.)	TOP BIWABIK (FT.)	ELEV (FT.)	THICK. BIWABIK (FT.)	TOP VA FM (FT.)	ELEV (FT.)	THICK. VA FM (FT.)
26010	1602	50NW	620	415	1284						415	1284	>157
26011	1602		455	445	1157						445	1157	>10
26013	1610	60NW	740	533	1148			738	971	>2	533	1148	179
26015	1605	50NW	893	595	1149			885	927	>6	595	1149	228
26017	1605		861	793	812						793	812	>68
26021	1605		608	T-1							T-1		
26023	1605		725	597	1008						597	1008	>128
26026	1614		715	692	922						692	922	>23
26028	1600	50NW	381	330	1347						330	1347	>39
26032	1611		690	598	1013						598	1013	>92
26033	1614		1104	1032	582			1096	518	>8	1032	582	64
26035	1600		915	T-VF				854	746	>61	T-VF		>854
26037	1605	45NW	301	83	1546						83	1546	>154
26038	1613		405	281	1332						281	1332	>124
26039	1606		956	802	804						802	804	>154
26041	1613		387	306	1307						306	1307	>81
26044	1612		205	T-1							T-1		
26046	1603		945	868	735						868	735	>77
26047	1609		800	736	873						736	873	>64
26057	1599		608	555	1044						555	1044	>53
26059	1603		608	497.5	1105.5						497.5	1105.5	>110.5
26060	1610		812	592	1018			719	891	>93	592	1018	127
26076	1610		1180	456	1154	1163	447	712	898	468	456	1154	256
26077	1609		374	171	1438						171	1438	>203
26079	1597		864	778	819			841	756	>23	778	819	63
26085	1606		535	479	1127						479	1127	>56
26086	1617		574	498	1119						498	1119	>76
26091	1609		231	156	1453						156	1453	>75
26092	1613		376	283.5	1329.5						283.5	1329.5	>92.5
26095	1605		425	249.5	1355.5						249.5	1355.5	>175.5
26096	1625		883	795	830						795	830	>88
26098	1604		755	702	902			738	866	>17	702	902	36
26099	1623		565	488	1135						488	1135	>77
26100	1613		465	412.5	1200.5						412.5	1200.5	>52.5
26101	1607		655	601	1006						601	1006	>54
26105	1617	45NW	212	85	1557						85	1557	>90
26108	1617	45NW	167	99	1547						99	1547	>48
26109	1612	45NW	242	216	1459						216	1459	>18
26110	1621	45NW	162	T-1							T-1		
26111	1613	45NW	162	T-1							T-1		
26112	1614	45NW	222	209	1466						209	1466	>9
26113	1621	45NW	214	194	1484						194	1484	>14
26114	1617	40NW	293	271	1443						271	1443	>14
26118	1618		1145	1101	517			1128	490	>17	1101	517	27
26127	1629		918	T-1							T-1		
26128	1632		1008	834	798			947	685	>61	834	798	113

DRILL HOLE #	TOP OF UNIT I (FT.)	ELEV. (FT.)	THICK. OF UNIT I (FT.)	TOP OF UNIT II (FT.)	ELEV. (FT.)	THICK. OF UNIT II (FT.)	TOP OF UNIT III (FT.)	ELEV. (FT.)	THICK. OF UNIT III (FT.)	TOP OF UNIT IV (FT.)	ELEV. (FT.)	THICK. OF UNIT IV (FT.)
26010	T-1		>415									
26011	T-1		>445									
26013	83	1538	>450	T-2		>83						
26015	256	1409	339	58	1560	198	T-3		>58			
26017	319	1286	474	70	1535	249	T-3		>70			
26021	81.5	1523.5	>526.5	T-2		>81.5						
26023	208	1397	389	T-2		>208						
26026	269	1345	423	84	1530	185	T-3		>84			
26028	T-1		>330									
26032	217	1394	381	T-2		>217						
26033	554	1060	478	421	1193	133	240.5	1373.5	180.5	T-4		>240.5
26035												
26037	T-1		>83									
26038	T-1		>281									
26039	323	1283	479	105.5	1500.5	217.5	T-3		>105.5			
26041	T-1		>306									
26044	T-1		>205									
26046	466	1137	402	276	1327	190	61	1542	215	T-4		>61
26047	202	1407	534	69	1540	133	T-3		>69			
26057	91	1508	464	T-2		>91						
26059	T-1		>497.5									
26060	99	1511	493	T-2		>99						
26076	T-1		>456									
26077	T-1		>171									
26079	363	1234	415	179	1418	184	T-3		>179			
26085	T-1		>479									
26086	117	1500	381	T-2		>117						
26091	T-1		>156									
26092	T-1		>283.5									
26095	T-1		>249.5									
26096	420	1205	375	145	1480	275	T-3		>145			
26098	154	1450	548	T-2		>154						
26099	51	1572	437	T-2		>51						
26100	T-1		>412.5									
26101	85	1522	516	T-2		>85						
26105	T-1		>85									
26108	T-1		>99									
26109	T-1		>216									
26110	T-1		>162									
26111	T-1		>162									
26112	T-1		>209									
26113	T-1		>194									
26114	T-1		>271									
26118	640.5	977.5	460.5	400	1218	240.5	245	1373	155	T-4		>245
26127	230	1399	404	T-2		>230						
26128	530	1102	304	309	1323	221	164	1468	145	T-4		>164

APPENDIX B

Geostatistical Data

DATA SOURCES

There are five sources of data for the Dunka Road geostatistical analysis: two mineralized assay files, a basic geologic report (with subsequent modifications), hand-drawn geologic cross-sections (subsequently computer drawn), and lengthy discussions with the NRRI project geologists.

Due to ongoing research and analysis at the Dunka Road site, the available data is encountering continuous change. The following sections present the details of the data used in this analysis. Every effort was made to include the most complete and most up-to-date information; nonetheless, this report is static while the interest in Dunka Road goes on.

FLECK RESOURCES ASSAY DATABASE

The main source of the quantitative data used in this analysis is the spreadsheet file (Appendix C). This spreadsheet file contains 1890 assay records from 84 separate drill holes. Each record is comprised of the 15 fields: a hole identification, seven geometric variables, and seven separate elemental assays. This data set includes NRRI assays of previously unsplit sulfide zones. The spreadsheet file (Appendix C) is called DUNKFLEK.WK1.

- *HOLE ID* - The hole identification numbers were generated by USX during the original exploration campaign. The numbers include most values, but not all, between 26010 and 26143.

- *COLLAR NORTHING* - The collar northing were originally UTM coordinates surveyed by USX. These UTM coordinates range between 5,272,000 to 5,276,000. To reduce data manipulation difficulties, a local coordinate system northing was generated by subtracting 5,270,000 from all collar northings. As such, the collar northings in this file vary from 2,510 to

5,023.

- *COLLAR EASTING* - The collar eastings were originally UTM coordinates surveyed by USX. These UTM coordinates varied between 575,000 to 580,000. As with the collar northing, a local coordinate system easting was generated by subtracting 570,000 from all collar eastings. As such, the collar eastings in this file vary from 5,040 to 9,300.

- *COLLAR ELEVATION* - The collar elevations are expressed as distance above mean sea level as surveyed by USX. Unlike the collar northings and eastings, the collar elevations were not modified in the local coordinate system.

- *HOLE DIP AT THE COLLAR* - The dip of the holes at the collars are expressed in degrees from horizontal. Of the 84 holes included in the analysis, 72 are vertical (dip = 90E). The reported dip of the 12 non-vertical holes vary from 40 deg. to 50 deg.

- *DIP DIRECTION AT THE COLLAR* - The dip directions at the collar are expressed as azimuths.

- *BEGINNING OF ASSAY INTERVAL ("FROM")* - The beginning of the assay intervals are the distances from the collars, along the cores, to the beginning of the assayed intervals.

- *END OF ASSAY INTERVAL ("TO")* - The end of the assay intervals are the distances from the collars, along the cores, to the end of the assayed intervals. Thus, the end minus the beginning yields the length of the assay interval.

- *COPPER* - The copper assays are given in percent Cu.

- *NICKEL* - The nickel assays are given in percent Ni.

- *SILVER* - The silver assays are given in ppm Ag.

- *GOLD* - The gold assays are given in ppb Au.

- *PLATINUM* - The platinum assays are given in ppb Pt.

- *PALLADIUM* - The palladium assays are given in ppb Pd.

- *RHODIUM* - The rhodium assays are given in ppb Rh.

This spreadsheet file contains all of the assay data used in the geostatistical analysis

presented in this report.

USX ASSAY DATABASE

A secondary source of quantitative data is the spreadsheet file DUNKAUSX.WK1 supplied by Steve Hauck of NRRI in early January 1990:

DUNKAUSX.WK1 389335 02 Jan 90

This spreadsheet file contains 2,023 assay records from 84 separate drill holes. Each record is comprised of the 15 fields: a sort number, a hole identification, eight geometric variables, and five separate elemental assays.

- *SORT NUMBER* - The sort number merely assigns a unique number to each record: starting at 1 and continuing to 2023.
- *HOLE ID* - Same as DUNKFLEK.WK1.
- *COLLAR NORTHING* - Same as DUNKFLEK.WK1.
- *COLLAR EASTING* - Same as DUNKFLEK.WK1.
- *COLLAR ELEVATION* - Same as DUNKFLEK.WK1.
- *HOLE DIP AT THE COLLAR* - Same as DUNKFLEK.WK1.
- *DIP DIRECTION AT THE COLLAR* - Same as DUNKFLEK.WK1.
- *BEGINNING OF ASSAY INTERVAL ("FROM")* - Same as DUNKFLEK.WK1.
- *END OF ASSAY INTERVAL ("TO")* - Same as DUNKFLEK.WK1.
- *COPPER* - Same as DUNKFLEK.WK1.
- *NICKEL* - Same as DUNKFLEK.WK1.
- *SULFUR* - The sulfur assays are given in percent S.
- *TOTAL FE* - The iron assays are given in percent Fe.
- *COBALT* - The cobalt assays are given in percent Co.

QUALITATIVE GEOLOGIC INFORMATION

Severson's (1988) report serves as a basis for the regional geologic interpretation behind the geostatistical analysis presented in this report. In addition, the manual interpretations presented on five geologic cross-sections and one plan map were used throughout the analysis (Plates 2-7).

IDENTIFICATION OF HOLES USED IN THE ANALYSIS

Hole	#[1]	Elev	North	East	Dip	Azi	TD[2]
26010	23	1602	3927	6882	50	315	620
26011	36	1602	3927	6882	90	0	455
26013	32	1610	4386	7502	60	333	740
26015	37	1605	4134	7200	50	330	893
26017	38	1605	4134	7200	90	0	861
26021	26	1606	3877	6909	90	0	608
26022	9	1605	3721	6199	90	0	606
26023	38	1605	3619	6255	90	0	725
26024	2	1605	3836	6147	90	0	586
26025	26	1613	2983	5618	90	0	1042
26026	19	1614	3727	6533	90	0	715
26027	38	1606	3237	6116	90	0	910
26028	18	1600	3969	6858	50	327	381
26030	16	1622	3712	7013	90	0	1094
26031	17	1599	3987	7295	90	0	1116
26032	8	1611	4532	7913	90	0	690
26033	20	1614	4241	7593	90	0	1104
26036	27	1596	4893	9300	90	0	1237
26038	13	1613	4386	7262	90	0	405
26039	30	1606	3901	7100	90	0	956
26041	33	1613	4284	7101	90	0	387
26042	2	1595	3540	7122	90	0	1946
26043	1	1606	4074	7704	90	0	1559
26044	11	1612	4357	7283	90	0	205
26045	17	1598	3663	6767	90	0	926
26046	11	1603	4197	7286	90	0	945
26047	18	1609	4367	7751	90	0	800
26049	5	1608	4366	8033	90	0	1207
26051	22	1600	4220	7854	90	0	1454
26052	1	1593	4091	8220	90	0	1866
26053	27	1595	3567	6639	90	0	1018
26054	44	1598	3288	6331	90	0	776
26056	43	1592	3140	6414	90	0	1693
26057	15	1599	3854	6662	90	0	608
26058	19	1612	3483	6434	90	0	817
26059	37	1603	4093	7001	90	0	608
26060	34	1610	4386	7502	90	0	812
26062	16	1593	3532	6868	90	0	1477
26064	5	1595	3746	7198	90	0	1496
26076	36	1610	4795	8428	90	0	1180
26077	14	1609	4258	6895	90	0	374
26078	36	1613	3639	6457	90	0	904

[1] "#" is the number of composites generated for this hole.

[2] "TD" is the total depth of the hole.

IDENTIFICATION OF HOLES USED IN THE ANALYSIS (con't)

Hole	#	Elev	North	East	Dip	Azi	TD
26079	27	1597	3587	6667	90	0	864
26080	3	1597	2630	5040	90	0	1925
26081	2	1578	2807	6640	90	0	2345
26082	42	1607	3472	6202	90	0	935
26083	46	1607	3251	5869	90	0	644
26084	3	1613	3107	5537	90	0	1354
26085	19	1606	3896	6419	90	0	535
26086	34	1617	4902	8810	90	0	574
26090	28	1595	3308	6549	90	0	1775
26091	14	1609	4099	6770	90	0	231
26092	25	1613	4024	6550	90	0	376
26093	23	1613	3092	5976	90	0	1085
26095	22	1605	4178	6947	90	0	425
26096	26	1625	4774	8673	90	0	883
26098	29	1604	3728	6406	90	0	755
26099	27	1623	4974	9054	90	0	564
26100	35	1613	3936	6603	90	0	465
26101	47	1607	3809	6475	90	0	655
26103	28	1612	3561	6510	90	0	965
26105	11	1617	4996	8760	45	325	212
26108	9	1617	4943	8675	45	325	167
26109	14	1612	4893	8593	45	335	242
26110	10	621	4855	8621	45	340	162
26111	15	1613	4903	8709	45	340	162
26112	18	1614	4943	8792	45	325	222
26113	16	1621	5008	8899	45	340	214
26114	14	1617	5023	9023	40	345	293
26115	12	1592	3421	7207	90	0	2180
26116	5	1610	3394	7451	90	0	2245
26118	47	1618	4621	8347	90	0	1145
26119	16	1568	3411	8140	90	0	2647
26120	1	1597	4467	8451	90	0	1080
26121	36	1594	3117	6668	90	0	2151
26122	6	1607	3689	7731	90	0	2242
26123	27	1597	3223	6863	90	0	2253
26124	48	1593	3354	6991	90	0	2415
26125	10	1597	3531	7841	90	0	2504
26127	30	1629	4927	8956	90	0	918
26128	30	1632	4824	8762	90	0	1008
26141	46	1592	3062	6230	90	0	1585
26142	24	1593	2907	6334	90	0	2118
26143	45	1592	2510	6197	90	0	2125